MOLECULAR AND CELLULAR BIOLOGY, Apr. 1998, p. 2309–2323 Vol. 18, No. 4
0270-7306/98/$04.00+0

Ca^{2+} Content and Expression of an Acidocalcisomal Calcium Pump Are Elevated in Intracellular Forms of *Trypanosoma cruzi*

HONG-GANG LU,[1] LI ZHONG,[1] WANDERLEY DE SOUZA,[2,3] MARLENE BENCHIMOL,[2]† SILVIA MORENO,[1] AND ROBERTO DOCAMPO[1]*

Laboratory of Molecular Parasitology, Department of Pathobiology, University of Illinois at Urbana-Champaign, Urbana, Illinois 61802,[1] and Laboratório de Biologia Celular e Tecidual, Universidade Estadual do Norte Fluminense, Campos,[2] and Instituto de Biofísica Carlos Chagas Filho, Universidade Federal do Rio de Janeiro, Ilha do Fundão, 21941 Rio de Janeiro,[3] RJ, Brazil

Received 28 October 1997/Returned for modification 22 December 1997/Accepted 21 January 1998

The survival of a eukaryotic protozoan as an obligate parasite in the interior of a eukaryotic host cell implies its adaptation to an environment with a very different ionic composition from that of its extracellular habitat. This is particularly important in the case of Ca^{2+}, the intracellular concentration of which is 3 orders of magnitude lower than the extracellular value. Ca^{2+} entry across the plasma membrane is a widely recognized mechanism for Ca^{2+} signaling, needed for a number of intracellular processes, and obviously, it would be restricted in the case of intracellular parasites. Here we show that *Trypanosoma cruzi* amastigotes possess a higher Ca^{2+} content than the extracellular stages of the parasite. This correlates with the higher expression of a calcium pump, the gene for which was cloned and sequenced. The deduced protein product (Tca1) of this gene has a calculated molecular mass of 121,141 Da and exhibits 34 to 38% identity with vacuolar Ca^{2+}-ATPases of *Saccharomyces cerevisiae* and *Dictyostelium discoideum*, respectively. The *tca1* gene suppresses the Ca^{2+} hypersensitivity of a mutant of *S. cerevisiae* that has a defect in vacuolar Ca^{2+} accumulation. Indirect immunofluorescence and immunoelectron microscopy analysis indicate that Tca1 colocalizes with the vacuolar H^+-ATPase to the plasma membrane and to intracellular vacuoles of *T. cruzi*. These vacuoles were shown to have the same size and distribution as the calcium-containing vacuoles identified by the potassium pyroantimoniate-osmium technique and as the electron-dense vacuoles observed in whole unfixed parasites by transmission electron microscopy and identified in a previous work (D. A. Scott, R. Docampo, J. A. Dvorak, S. Shi, and R. D. Leapman, J. Biol. Chem. 272:28020–28029, 1997) as being acidic and possessing a high calcium content (i.e., acidocalcisomes). Together, these results suggest that acidocalcisomes are distinct from other previously recognized organelles present in these parasites and underscore the ability of intracellular parasites to adapt to the hostile environment of their hosts.

Trypanosoma cruzi is an obligate intracellular protozoan parasite that infects a wide variety of vertebrates and is the etiologic agent of Chagas' disease in humans. The life cycle of *T. cruzi* involves several different stages. The epimastigotes proliferate within the gut of reduviid insects and then transform into nondividing, but highly infective, metacyclic trypomastigote forms, which are released into the urine and feces and inoculated into the vertebrate host. In this host, the trypomastigotes invade different cell types, remain in an acidic parasitophorous vacuole for a few hours, and then disrupt the vacuolar membrane and gradually transform into amastigote forms, which actively reproduce in direct contact with the cytoplasm of the host cell. Subsequently, the amastigotes transform into trypomastigotes which are released from the host cells and reach the bloodstream, from which they are taken up by the vectors (12, 35).

Ca^{2+} signaling has been shown to play a key role in the process of mammalian cell invasion and the intracellular development of this parasite. An increase in the cytosolic Ca^{2+} concentration ($[Ca^{2+}]_i$) of *T. cruzi* trypomastigotes occurs upon invasion (13, 31), and pretreatment of the trypomastigotes with intracellular Ca^{2+} chelators—the tetraacetoxymethyl esters of (bis)-*o*-aminophenoxy)-ethane-*N*,*N*,*N*′,*N*′-tetraacetic acid (BAPTA) and 2-{[2-bis(carboxymethyl)-amino-5-methylphenoxyl]-methyl}-6-methoxy-8-bis(carboxymethyl)-aminoquinoline (QUIN-2)—to prevent the increase in $[Ca^{2+}]_i$ results in an inhibition of cellular invasion (31, 66).

Two large Ca^{2+} sinks, the extracellular space and the endoplasmic reticulum, are important sources of Ca^{2+} for calcium signaling in most eukaryotic cells (8). However, *T. cruzi* amastigotes are not in contact with the extracellular space because they live in the cytosol, where the free calcium concentration is very low (of the order of 0.1 μM) compared to that of the extracellular space (of the order of 1 mM). This dramatic difference in external free calcium suggests that intracellular stores must be very important in the regulation of Ca^{2+} homeostasis in the amastigotes.

In contrast to mammalian cells, the different stages of *T. cruzi* possess most of their intracellular Ca^{2+} in an acidic compartment named the acidocalcisome (14). The biochemical characterization of this organelle has provided evidence that it is acidified by a vacuolar-type proton-translocating ($V\text{-}H^+$) ATPase and that it has a Ca^{2+}/H^+ countertransporting ATPase for Ca^{2+} uptake (14). Acidocalcisomes have also been found in other trypanosomatids, such as *Trypanosoma brucei* (43, 58, 59) and *Leishmania mexicana amazonensis* (28), and in *Toxoplasma gondii* (32). This organelle is in various aspects similar to the vacuole present in fungi and plant cells (62) but apparently has no counterpart in mammalian cells. The use of

* Corresponding author. Mailing address: Laboratory of Molecular Parasitology, Department of Pathobiology, University of Illinois, 2001 S. Lincoln Ave., Urbana, IL 61802. Phone: (217) 333-3845. Fax: (217) 244-7421. E-mail: rodoc@uiuc.edu.

† Present address: Universidade Santa Ursula, Botafogo, Rio de Janeiro, CEP 22231-010, Brazil.

quick freezing, ultracryomicrotomy, and electron probe microanalysis to study the elemental composition of different compartments in *T. cruzi* epimastigotes with or without prior treatment with ionophores has recently provided evidence (44) that acidocalcisomes correspond to the electron-dense vacuoles previously described for these parasites (15).

In mammalian cells, Ca^{2+} has also been reported to be present in acidic organelles carrying vacuolar-type proton pumps, such as endosomes, lysosomes, and the trans-Golgi network, and secretory granules such as chromaffin, pancreatic zymogen, and atrium-specific granules (19, 37, 50, 61), but the functional significance of the high Ca^{2+} content of these organelles is unknown (37). Recent evidence has indicated, however, that second messengers such as inositol 1,4,5-trisphosphate and cyclic ADP ribose can release Ca^{2+} from pancreatic zymogen granules (19), although this conclusion is disputed by other investigators (57). The mechanism of Ca^{2+} uptake might not be the same in all these organelles. In fact, zymogen granules seem to acquire their Ca^{2+} together with the proteins from the Golgi complex, whereas chromaffin granules seem to be endowed with a specific Ca^{2+}/Na^{+} antiport (37). Except for a Ca^{2+}-ATPase that was purified from rat liver lysosomes (16) and a Ca^{2+}-ATPase gene that was cloned from rat stomach tissue (21) and that exhibits 50% amino acid identity with the Golgi complex-located *PMR1* gene product of *Saccharomyces cerevisiae* (2, 38), no studies have been carried out yet to investigate the presence of specific Ca^{2+}-translocating ATPases in most of these organelles.

This study provides further evidence that acidocalcisomes are organelles distinct from lysosomes and other previously recognized organelles present in these parasites. It also reports the identification in *T. cruzi* of the *tca1* gene, which encodes a protein with homology to mammalian plasma membrane Ca^{2+}-ATPases (PMCA) but with characteristics that place it in a novel category of Ca^{2+}-ATPases along with the vacuolar Ca^{2+}-ATPases described for *S. cerevisiae* (9) and *Dictyostelium discoideum* (30). Indirect immunofluorescence and immunoelectron microscopy analysis suggest that the product of this gene (Tca1) is associated not only with the plasma membrane but also with the acidocalcisomes. The gene is expressed at a high level in the amastigote stages that contain an elevated Ca^{2+} concentration and a larger number of acidocalcisomes compared to other stages of the parasite and is able to functionally complement the *PMC1* gene, encoding the vacuolar Ca^{2+}-ATPase of *S. cerevisiae.*

MATERIALS AND METHODS

Culture methods. *T. cruzi* trypomastigotes and amastigotes (Y strain) were obtained from the culture medium of L_6E_9 myoblasts by a modification of the method of Schmatz and Murray (42) as we have described before (14). The final concentration of trypomastigotes and amastigotes was determined with a Neubauer chamber. The contamination of trypomastigotes with amastigotes and intermediate forms or of amastigotes with trypomastigotes and intermediate forms was always less than 5%. *T. cruzi* epimastigotes (Y strain) were grown at 28°C in a liquid medium consisting of brain heart infusion (37 g/liter), hemin chlorohydrate (20 mg/liter dissolved in 50% triethanolamine), and 10% heat-inactivated newborn calf serum (14). Five days after inoculation, cells were collected by centrifugation. The protein concentration was determined by the biuret assay (20) in the presence of 0.2% deoxycholate. L_6E_9 myoblasts were cultured as described before (33). Yeast strains K665 *MAT***a** (*vcx1::hisG pmc1::TRP1*) and K661 *MAT***a** (*vcx1::hisG*), kindly provided by Kyle W. Cunningham, Department of Biology, The Johns Hopkins University, Baltimore, Md. (10), were grown at 30°C in standard YPD medium (1% Difco yeast extract, 2% Bacto Peptone, 2% dextrose) or in YPD medium, pH 5.5 (adjusted with succinic acid), supplemented with 200 mM $CaCl_2$. Cell growth was assessed by measuring the optical density of the liquid cultures at 600 nm (see Fig. 5B) or by counting the number of colonies in plates (see Fig. 5A). Both strains are isogenic and harbor the following additional mutations: *ade2-1*, *can1-100*, *his3-11*, *15 leu2-3*, *112 trp1-1*, and *ura3-1.*

Chemicals. Fetal and newborn calf serum, Dulbecco's phosphate-buffered saline (PBS), Tween 20, Triton X-100, arsenazo III, EGTA, and poly-L-lysine (molecular weight, 70,000) were purchased from Sigma Chemical Co. Fluorescein- and rhodamine-labeled antibodies were from Molecular Probes, Inc., Eugene, Oreg. Trizol reagent and *Taq* polymerase were from Gibco BRL, Life Technologies Inc., Grand Island, N.Y. The Poly(A)Tract mRNA isolation system, lambda EMBL3 phage, restriction enzymes, and pGEM-T vectors were from Promega (Madison, Wis.). Sequenase was from United States Biochemical Corporation (Cleveland, Ohio). The pET-28a expression vector and the *Escherichia coli* DE3 strain were from Novagen (Madison, Wis.). The pYES2 vector was from Stratagene (La Jolla, Calif.). Monoclonal antibody N-2 against the 110-kDa accessory protein of the $V\text{-}H^{+}$-ATPase was purchased from the Monoclonal Antibody Center of the University of Hawaii through Agnes Fok. Polyclonal antibodies against *T. cruzi* cruzipain were kindly provided by Juan Jose Cazzulo (University of San Martin, San Martín, Argentina). Gold-labeled goat anti-rabbit antibodies were obtained from Ted Pella, Inc., Reddington, Calif. Biotin succinimidyl ester and the enhanced chemiluminescence (ECL) detection kit were from Amersham Life Sciences, Inc., Arlington Heights, Ill. All other reagents were analytical grade.

Nucleic acid analysis. DNA was isolated by standard procedures (39). Total RNA was isolated with Trizol reagent according to the manufacturer's recommendations. The polyadenylated RNA was obtained with the Poly(A)Tract mRNA isolation system. DNA was run in 0.8% agarose gels with TBE (9.5 mM Tris-boric acid, 2.0 mM EDTA, pH 8.0) buffer. RNA was electrophoresed in 1% agarose gels with 2.2 M formaldehyde, 100 mM MOPS (morpholinepropanesulfonic acid), 40 mM sodium acetate, and 5 mM EDTA (pH 8.0) (39). Southern and Northern hybridizations were done by standard procedures (39). All the probes for hybridization were labeled with [^{32}P]dCTP by using random hexanucleotide primers. The hybridized filters were washed under high-stringency conditions (0.1% standard saline citrate–0.1% sodium dodecyl sulfate [SDS] at 65°C), unless otherwise indicated. Oligonucleotide primers were designed to recognize the ATP phosphorylation site and the ATP-binding site of cationic ATPase genes (1, 36), i.e., 5′CGGGATCCGTNATNTGYWSNGAYAA3′ and 5′CGGAATTCGSRTCRTTNRYNCCR3′ (where N is A + T, Y is C + T, W is A + T, S is G + C, and R is A + G) as the 5′ primer and the 3′ primer, respectively. PCR was performed in a PTC-100 programmable thermal controller (MJ Research, Inc., Watertown, Mass.) at 94°C for 1 min, 55 to 72°C for 2 min, and 72°C for 2 min/cycle (30 cycles) with *Taq* polymerase. PCR products were cloned into the pGEM-T vector according to the manufacturer's instructions. The cloned PCR products were sequenced, and the deduced amino acid sequences were compared with the database in GenBank. A ~1.0-kb PCR clone with identity to organelle-type Ca^{2+}-ATPases was used to screen a genomic DNA library of *T. cruzi*. The library was constructed in lambda EMBL3 phage with 9- to 23-kb *Bam*HI fragments of genomic DNA from *T. cruzi* epimastiotes according to the manufacturer's instructions. DNA sequencing was performed by the dideoxynucleotide chain termination method of Sanger et al. (40) either manually or with a 373A DNA automatic sequencer (Perkin-Elmer Applied Biosystems, Foster City, Calif.). Internal oligonucleotide primers were designed to complete the DNA sequence in both directions. DNA and deduced amino acid sequence analyses were performed with the University of Wisconsin Genetics Computer Group software package (GCG program, version 8.0). Hydropathy analysis was done with the Gene Jockey sequence processor (Biosoft, Cambridge, United Kingdom). The *TcP0* fragment used as a control in Northern blots (see Fig. 3) was obtained by amplifying *T. cruzi* genomic DNA by the PCR technique, with primers corresponding to nucleotides 3 to 54 and 918 to 936 in the sequence of the *TcP0* gene (47). Densitometric analysis of Northern blots was done with an ISI-1000 digital imaging system (Alpha Inotech Corp.). Comparison of levels of *tca1* transcripts between the different stages was done by taking as a reference the densitometric values obtained with the *TcP0* transcripts and assuming a similar level of expression of this gene in all stages (47). Similar results were obtained when the densitometric values were compared by taking into account the amount of RNA added to each lane in four different experiments.

Preparation of antibodies. A DNA fragment encoding the 174-amino-acid COOH-terminal domain of the Tca1 protein was removed by *Nde*I and *Bgl*II double digestion from plasmid p*tca1* containing the complete *tca1* gene. The fragment was subcloned into the *Nde*I and *Bam*HI sites of the pET-28a expression vector, resulting in a construct that encoded the protein fused to a six-histidine tag that allowed its purification on nickel-agarose columns. This plasmid was checked by DNA sequencing to ensure that the correct construct had been obtained. The recombinant plasmid was transfected into the DE3 strain of *E. coli*, the fusion protein was induced, and the expressed protein of about 33 kDa, present in inclusion bodies, was solubilized and purified according to the manufacturer's instructions. Rabbits were injected subcutaneously with 100 μg of fusion protein emulsified in Freund's complete adjuvant, followed 2 weeks later by subcutaneous injection of 100 μg of fusion protein in Freund's incomplete adjuvant. At 6, 8, and 10 weeks following the initial injection, rabbits were boosted with 100 μg of fusion protein in PBS containing a 10-mg/ml suspension of $A1(OH)_3$. Serum was collected before the initial injection (preimmune serum) and 10 days after each boost. The antiserum was aliquoted and stored at −70°C. Affinity purification of anti-Tca1 antibody was performed as described elsewhere (39). Briefly, 500 μg of fusion protein was fractionated by SDS-polyacrylamide

gel electrophoresis and transferred to nitrocellulose paper. After being blocked with 5% nonfat dry milk in TBST (10 mM Tris-HCl [pH 8.0], 150 mM NaCl, 0.05% Tween 20), the paper was incubated with the anti-Tca1 serum to bind the specific antibody to Tca1 protein. Then the paper was washed three times with TBST, and antibody was eluted from the nitrocellulose paper with elution buffer (0.2 M glycine [pH 2.8], 1 mM EDTA).

SDS electrophoresis and preparation of Western blots. The electrophoretic system used was essentially the same as that described by Laemmli (25). *T. cruzi* epimastiotes (2.5×10^8), trypomastigotes (1×10^9), or amastigotes (1×10^9) were centrifuged at $1,000 \times g$ for 10 min, resuspended in 300 μl of Dulbecco's PBS containing proteinase inhibitors (1 μg of aprotinin per ml, 1 μg of leupeptin per ml, 1 μg of pepstatin per ml, and 1 mM phenylmethylsulfonyl fluoride), and frozen at −70°C. Cells were thawed and homogenized with a Teflon pestle at 4°C. Aliquots of different stages of *T. cruzi* (10 μl; about 20 μg of protein) were mixed with 10 μl of 125 mM Tris-HCl (pH 7)–10% (wt/vol) β-mercaptoethanol–20% (vol/vol) glycerol–4.0% (wt/vol) SDS and 4.0% (wt/vol) bromophenol blue as tracking dye and boiled for 5 min prior to application to SDS–7.5% polyacrylamide gels. Electrophoresed proteins were transferred to nitrocellulose by the method of Towbin et al. (56), with a Bio-Rad Laboratories (Richmond, Calif.) Transblot apparatus. Following transfer, the nitrocellulose was blocked in 5% nonfat dry milk in TBST overnight at 4°C. A 1:1,000 dilution of polyclonal antiserum in blocking buffer was then applied at room temperature for 60 min. The nitrocellulose was washed three times for 15 min each with TBST. Immunoblots were visualized on radiographic film (Kodak) with the ECL chemiluminescence detection kit and according to the instructions of the manufacturer (Amersham Life Sciences).

Functional complementation of the *PMC1* gene of *S. cerevisiae* with *tca1*. We transformed the *S. cerevisiae vcx1 pmc1* strain K665 with the yeast expression vectors pYES2 and pYES2-*tca1* by electroporation. The Ura^+ transformants were selected by plating on synthetic-complete Ura medium (10). The *tca1* coding region was amplified by the PCR technique from a lambda clone containing the complete *tca1* gene and a *Hin*dIII site created on the PCR primers. The *tca1* coding region was placed at the *Hin*dIII site of pYES2 with the same orientation as the *GAL1* promoter. The cultures were grown in YPD medium (pH 5.5) containing 200 mM $CaCl_2$ to identify Ca^{2+}-tolerant transformants.

Immunofluorescence microscopy. Parasites fixed with 4% formaldehyde were allowed to adhere to poly-L-lysine-coated coverslips, permeabilized with 0.3% Triton X-100 for 3 min, blocked with 3% bovine serum albumin in PBS, and prepared for immunofluorescence with a 1:100 or 1:200 (see Fig. 8) dilution of the antibody against the 33-kDa expressed protein or a 1:25 dilution of the monoclonal antibody against the 110-kDa accessory protein of the $V\text{-}H^+$-ATPase and a rhodamine- or fluorescein isothiocyanate-coupled goat anti-rabbit immunoglobulin G (IgG) secondary antibody (1:80), respectively. Control preparations were incubated with preimmune serum or without the primary antibody. Immunofluorescence images were obtained with an Olympus BX-60 fluorescence microscope. The images were collected with a system consisting of a charge-coupled device camera (model CH250; Photometrics Ltd., Tucson, Ariz.), an electronic unit (model CE 200A, equipped with a 50-Hz 16-bit A/D converter), and a controller board (model NU 200; both from Photometrics Ltd.). Images were acquired and evaluated by a software package (Adobe Photoshop) on a Macintosh Quadra 840 AV computer (Apple Computer, Inc., Cupertino, Calif.). In experiments aiming at the colocalization of Ca^{2+}- and H^+-ATPases, the samples were examined in a Zeiss LSM10 laser scanning confocal microscope. Optical sections of 0.1 μm were used.

Electron microscopy. For imaging whole cells (see Fig. 12), trypomastigotes were treated exactly as described by Dvorak et al. (15). Amastigotes were suspended in Dulbecco's PBS (pH 7.2). Drops were applied to Formvar- and carbon-coated 200-mesh copper grids, and cells were allowed to adhere for 10 min and then carefully blotted dry and observed directly with a Hitachi 600 transmission electron microscope operating at 100 kV.

For localization of calcium-containing sites (see Fig. 9), the potassium pyroantimoniate-osmium technique was used (3). The cells were fixed for 60 min at room temperature in a solution containing 2.5% glutaraldehyde in 0.1 M cacodylate buffer (pH 7.2), washed twice with 0.1 M cacodylate buffer and twice with 0.1 M potassium phosphate buffer (pH 7.2), and postfixed with 1% osmium tetroxide and 2% potassium pyroantimoniate for 1 h at 4°C. Potassium pyroantimoniate (Merck) was dissolved in distilled water to 5% (wt/vol), heated to boiling point, and cooled. The original volume was restored, and the solution was filtered to remove any precipitate (3, 24). The fixative solution was made by mixing 1 ml of 2% aqueous osmium tetroxide, 1 ml of 5% potassium pyroantimoniate, and 0.5 ml of 0.1 M potassium phosphate buffer. The pH of the mixture was adjusted to 7.5 to 7.8 with 0.1 N acetic acid in order to achieve efficient precipitation. After postfixation, the cells were washed in potassium phosphate buffer (pH 7.2), dehydrated in acetone, and embedded in Epon. Thin sections were collected on grids, lightly stained with lead citrate, and observed in a transmission electron microscope. In order to control the specificity of the technique, thin sections were exposed for 20 to 30 min at 60°C to 5 mM EGTA, washed with distilled water, and then observed.

For conventional electron microscopy (see Fig. 10), cells were fixed in 2.5% glutaraldehyde–0.1 M K^+-HEPES buffer (pH 7.5), for 40 min at room temperature and resuspended in 0.1 M K^+-HEPES buffer (pH 7.5)–50 mM sucrose, before postfixation in 2% OsO_4 in water with a microwave oven (Ted Pella model 3440): two treatments at 42°C (maximum), each for 8 s on, 20 s off, and 8 s on, with a 15-min incubation at room temperature after each treatment. Specimens were then en bloc stained with 3% potassium ferricyanide for 10 min, rinsed in water, incubated in saturated uranyl acetate for 30 min, dehydrated in ethanol-propylene oxide, and embedded in Lx112 Epon substitute. Ultrathin sections were made in a Reichert Ultracut E ultramicrotome, stained with uranyl acetate and lead citrate, and observed in a JEOL 100CX electron microscope operating at 80 kV.

For immunocytochemistry (see Fig. 7 and 11), two approaches were used. Initially, the cells were fixed for 60 min at 4°C in a solution containing 0.2% glutaraldehyde, 4% freshly prepared formaldehyde, and 0.8% picric acid in 0.1 M cacodylate buffer (pH 7.2). Fixed cells were washed in PBS–1% albumin and incubated for 60 min in the presence of 50 mM NH_4Cl, dehydrated at −20°C in an ethanol series, and infiltrated at the same temperature in Unicryl (41). Polymerization was carried out for 72 h at −20°C by UV irradiation. Thin sections were collected on 300-mesh nickel grids; incubated in the presence of the antibodies recognizing either Ca^{2+}-ATPase, H^+-ATPase, or cruzipain; washed in PBS-albumin; and then incubated in the presence of goat anti-mouse or anti-rabbit IgG labeled with 5- or 10-nm gold, washed in distilled water, stained with uranyl acetate and lead citrate, and observed in the transmission electron microscope. In a second approach, after fixation the cells were infused in a mixture of 25% polyvinylpyrrolidone and 2.3 M sucrose for 2 h and then plunged into liquid nitrogen (55); cryosections were then obtained at a temperature range of −80 to −100°C and collected on nickel grids coated with Formvar film and carbon. For immunolabeling, the cryosections were washed in PBS–3% albumin, quenched in 50 mM NH_4Cl for 30 min, and subsequently incubated for 3 h in the presence of the antibodies (1:50 or 1:100 dilution), washed, and incubated in the presence of 5- or 10-nm-gold-labeled goat anti-rabbit or anti-mouse IgG (1:50 dilution for 60 min). Then the specimens were thinly embedded in a 9:1 mixture of 3% polyvinyl alcohol and uranyl acetate (55) and observed with a Hitachi 600 transmission electron microscope operating at 100 kV. Controls were carried out with an unrelated antibody or with incubation in the presence of the secondary antibody only.

Cell surface labeling. Cell surface labeling was performed by a modification of the method of Hart et al. (22). Epimastigotes were washed three times with 10 mM sodium phosphate (pH 8.6)–150 mM NaCl–0.1 mM $MgCl_2$–0.1 mM $CaCl_2$ at room temperature and were then resuspended in 1 ml of the same ice-cold medium (4×10^6 cells/ml). Biotin succinimidyl ester (in dry dimethyl formamide) was added to the cells according to the instructions provided by Amersham and incubated for 1 h at 4°C with rotation. Cells were then washed three times with ice-cold Dulbecco's PBS and lysed in 0.5 ml of ice-cold immune precipitation buffer (1% Nonidet P-40, 20 mM Tris-HCl [pH 7.6], 0.1 mM EDTA, 1 mM phenylmethylsulfonyl fluoride, 2 μg of pepstatin per ml, 2 μg of leupeptin per ml, 1 μg of soybean trypsin inhibitor per ml). Cells were kept at 4°C for 30 min with rotation, and the lysate was centrifuged for 20 min at $10,000 \times g$. The supernatant was diluted to 1.5 ml with immunoprecipitation buffer containing 150 mM NaCl and precipitated with polyclonal anti-Ca^{2+}-ATPase antibody (1:300). After incubation for 16 h at 4°C, immunocomplexes were allowed to bind to protein A-Sepharose beads by incubating them for 1 h at 4°C. The beads were washed five times with immunoprecipitation buffer, and bound proteins were eluted in boiling SDS sample buffer. The proteins were separated on an SDS–10% polyacrylamide gel and blotted onto a nitrocellulose membrane as described above. The membrane was probed with avidin-peroxidase conjugate according to the protocol provided by Amersham. Proteins were visualized by ECL (Amersham).

Cell permeabilization. Variations in free Ca^{2+} concentrations in permeabilized cells were monitored by measuring the changes in the absorbance spectrum of arsenazo III (14), with the SLM Aminco DW2000 spectrophotometer at the wavelength pair of 675 and 685 nm.

Nucleotide sequence accession number. DNA sequence data was deposited in GenBank under accession no. U70620.

RESULTS

Cloning and characterization of a Ca^{2+}-ATPase gene. Since acidocalcisomes are in various respects similar to the vacuoles present in fungi and plant cells (62), we looked for the presence of a gene encoding a Ca^{2+}-ATPase with homology to the Ca^{2+}-ATPase present in the vacuole of *S. cerevisiae* (9) and in *D. discoideum* (30). Degenerate oligonucleotides corresponding to two conserved domains, a phosphorylation site and a site involved in ATP binding (1, 36), were used to amplify, by the PCR technique, specific sequences from *T. cruzi* genomic DNA. The PCR products were cloned and sequenced. Analysis of the deduced partial amino acid sequence of these clones revealed that a ~1.0-kb PCR clone had the best scores of sequence identity (31 and 37%) and similarity (50 and 55%)

A

```
     TTGAGATTGATGCGATAAACTCTTTCTCTCCTTATATATATATACATCTAATTATATCTTTTTGTGTGGCGACGTCATGCATGTATGCGT
     TTATACGAGTGTTTGTGTGTGCGTGTGTGTGTGTGTGTGTGTTTTTTTTTTGGTGCAGACGACATGTCTCTTCCTCTTTCTTTCTTTCT
     TTCTTTCTTTCTTTCTTTTTTTATTTATTTCTCATTCATGCCAATTTGTTACCATTACAACACCGCTTAGTACTGTACTTGAGGCATAAA
     CCGGGGAAAAAAGCAAAAAAAAAAAAAAAAAAAAAAAGAAAAAAAAAAAAAGAAAAGAAAAAAAAAAAAAAAAAGAAAAAAGAACAATAAAAAC
     GTAGGTTAGTAGCAAAACCAAATAAAAAGTGTGTATTTTTCAAATACGCAAGAGCTGTAAAAATATCTGTATTGTTGTCTGCTAAAATAC
     GGGCAGCGACATCATACACACACACGCATATTATTATTTTTCTTTCTCCTCCCCTCCCCTCTAGTTTTTTTTCTCACGCAAAAAGTGAAG
     ATGCGGAGATCATCTTTCTCCTATGGCTCGTGTGATGAAATGGAGGAGGAAACTAAGATGCGGCGATCTCGTCTGATGGAATCCGTCCGC  90
1    M  R  R  S  S  F  S  Y  G  S  C  D  E  M  E  E  E  T  K  M  R  R  S  R  L  M  E  S  V  R
     CGGAGAACCTCAATTCGTGTAAACTTTACAGACGGTGACGACGTCGGGGTGAGCATTCGAACGGATCTTGAAAATATATTTGCTCGTGCC  180
30   R  R  T  S  I  R  V  N  F  T  D  G  D  D  V  G  V  S  I  R  T  D  L  E  N  I  F  A  R  A
     AACGAGGGTATGCCGCTGTACGAGAAGTTGGGGAGGGCCGAGGGCATTGCCGCGAAGCTCCAGATGGACCTTAATAATGGTGTAAGAAGC  270
60   N  E  G  M  P  L  Y  E  K  L  G  R  A  E  G  I  A  A  K  L  Q  M  D  L  N  N  G  V  R  S
     GAAACTGTGGAACGGCGCCGTACCGTGTTTGGAAGGAACGAGCTGCCAGAGGAGGAGGAGCTATCTTTCTGGCGGATATACAAGGCGGCG  360
90   E  T  V  E  R  R  R  T  V  F  G  R  N  E  L  P  E  E  E  E  L  S  F  W  R  I  Y  K  A  A
     TGGAGTGACCAAATGATTCTTCTCCTCTCTGGCGCTGCATTTGTGTCGCTGGTGCTTGGTCTGACGGTTCCAGAGCCCGGCCGGGACAAG  450
120  W  S  D  Q  M  I  L  L  L  S  G  A  A  F  V  S  L  V  L  G  L  T  V  P  E  P  G  R  D  K
     GCGGACACGGGGACGGGGTGGATTGAGGGGTTTGCGATCTTAGTTTCCGTGCTTATTGTAACGACGGTGTCATCTGTAAATGACTACCGC  540
150  A  D  T  G  T  G  W  I  E  G  F  A  I  L  V  S  V  L  I  V  T  T  V  S  S  V  N  D  Y  R
     AAAGAGCTGAAGTTCCGCCAGTTGATGGAGGAGAACTCTGCGCAGCCGATCGCAGTGATTCGTGGCGGGCGTGAGCAGGTCATTGACGTG  630
180  K  E  L  K  F  R  Q  L  M  E  E  N  S  A  Q  P  I  A  V  I  R  G  G  R  E  Q  V  I  D  V
     ACGGAGATCGTTGTGGGGGATATTGTGAGTCTGTCGACTGGTCTCGTGGTGCCCGTGGACGGCTTTTACGTGCGCGGCCTCAGCGTGGTG  720
210  T  E  I  V  V  G  D  I  V  S  L  S  T  G  L  V  V  P  V  D  G  F  Y  V  R  G  L  S  V  V
     ATCGACGAAAGCAGCGTGACTGGGGAGAACGACCCAAAGAAGAAAGGTGTGCAGGCGCCGATCCTCCTGACTGGCACCGTTGTGAATACA  810
240  I  D  E  S  S  V  T  G  E  N  D  P  K  K  K  G  V  Q  A  P  I  L  L  T  G  T  V  V  N  T
     GCGGAGGACGCGTACATGCTTGCGTGTGCTGTGGGCGAGAGCTCGTTTGGCGGTAAACTGCTGATGGAGTCGCGACAGGAGGGTGGGCCA  900
270  A  E  D  A  Y  M  L  A  C  A  V  G  E  S  S  F  G  G  K  L  L  M  E  S  R  Q  E  G  G  P
     CGGATGACACCCCTGCAGGAGCGCCTGGACGAGCTTGCGGGGCTGATTGGCCGCTTTGGCATGGGAAGTGCGGTCCTTCTTTTCTCGTTG  990
300  R  M  T  P  L  Q  E  R  L  D  E  L  A  G  L  I  G  R  F  G  M  G  S  A  V  L  L  F  S  L
     CTGTCGCTTCTAGAGGTGTTTCGCATCATTCGTGGCACCGATGAATTCCACATGAAGACGTTCCTGGACCACTTTCTTCTGTGCGTCACG  1080
330  L  S  L  L  E  V  F  R  I  I  R  G  T  D  E  F  H  M  K  T  F  L  D  H  F  L  L  C  V  T
     ATCGTTGTTGTGGCTGTCCCGGAGGGACTGCCACTGGCTGTGACGATTGCACTTGCGTACTCGCAGAAGAAGATGCAGGAGGACAACAAC  1170
360  I  V  V  V  A  V  P  E  G  L  P  L  A  V  T  I  A  L  A  Y  S  Q  K  K  M  Q  E  D  N  N
     CAGGTGCGGCGCCTGTGTGCTTGTGAGACGATGGGGTGCGCGACGCAGATCTGCAGCGACAAGACCGGGACTCTGACGCAGAACCTGATG  1260
390  Q  V  R  R  L  C  A  C  E  T  M  G  C  A  T  Q  I  C  S  D  K  T  G  T  L  T  Q  N  L  M
     AGTGTGGTGCAGGGGTACATTGGGTTGCAGCGGTTCAATGTGCGCGACCCCGGGGACGTTCCGACGCCGATTGTGCTGCGGAATGTGCCG  1350
420  S  V  V  Q  G  Y  I  G  L  Q  R  F  N  V  R  D  P  G  D  V  P  T  P  I  V  L  R  N  V  P
     GCTGCGTCGCGGGATCTGCTGGTGGAGGGCCTGTCGCTCAACAGCTCGAGCGAGAAGGTGGTGTGTCGCACCGGCCGTGATGGGGAGTCT  1440
450  A  A  S  R  D  L  L  V  E  G  L  S  L  N  S  S  S  E  K  V  V  C  R  T  G  R  D  G  E  S
     GTGGCGCGACCCTACTGGCAGTGGCGGGCGGACAAGGGTAACAAGACGGACAATGCGCTGTTGGACTTTGTGGACCGTGTGCTGCTGCAG  1530
480  V  A  R  P  Y  W  Q  W  R  A  D  K  G  N  K  T  D  N  A  L  L  D  F  V  D  R  V  L  L  Q
     GACGGCGATCCCACTGACATGACGAGTCGCCCGCACCAGCGCGTGCGAGCGGGGTCGCGGCACGGCTTCGCCATCTTTCCTTTCACGAGC  1620
510  D  G  D  P  T  D  M  T  S  R  P  H  Q  R  V  R  A  G  S  R  H  G  F  A  I  F  P  F  T  S
     GAGCGGAAATTCATGAGCGTCGTTGTAGCCGGCCCGGGCGGTGTGCTGACTGCAGCACGTGAAGGGCGGGTCGGACCGCGTGCTGGAAAT  1710
540  E  R  K  F  M  S  V  V  V  A  G  P  G  G  V  L  T  A  A  R  E  G  R  V  G  P  R  A  G  N
     GTGCGACCGCTACGTTTCCGCTTCGGGTGCGGAGGAGGAGCCACTGACGGATGCGATGCGGACAAAGATCGTTGTGCAGATCCGTTCCCT  1800
570  V  R  P  L  R  F  R  F  G  C  G  G  G  A  T  D  G  C  D  A  D  K  D  R  C  A  D  P  F  P
     CCGCTAACGACGCGAACCGCACGATCGGTGTGGCTTATGGGCGTGTCGATGGCGAAGGCCTTCCCGCGAGCGAGCTACGGTGCCGCTGGT  1890
600  P  L  T  T  R  T  A  R  S  V  W  L  M  G  V  S  M  A  K  A  F  P  R  A  S  Y  G  A  A  G
     GTCGGTTGCGCTCGTGGGCATTCAGGACCCTCTGCGGCCGGAGGTACCAGACGCGGTGCGGAAGTGCAGCAAGCTGGAGTGACGGTGCGA  1980
630  V  G  C  A  R  G  H  S  G  P  S  A  A  G  G  T  R  R  G  A  E  V  Q  Q  A  G  V  T  V  R
     ATGTGCACCGGCGACAACCTGGACACGGCGGTGGCGATCTCGCGCAGTGCGCATTTACAACCGTTTACGTGGCGATGTGGCAATGACCGG  2070
660  M  C  T  G  D  N  L  D  T  A  V  A  I  S  R  S  A  H  L  Q  P  F  T  W  R  C  G  N  D  R
     AAGGAATTCCGCAGCCTTGTGTACGACGCTTACGGCAGCAGCGCTAACATGGAGAAGTTCTGGCCCATCCTTGACCGCATGGTGGTGATG  2160
690  K  E  F  R  S  L  V  Y  D  A  Y  G  S  S  A  N  M  E  K  F  W  P  I  L  D  R  M  V  V  M
     GCGCGCTCGCAGCCGCTGGACAAGCAGCTCCTGGTGCTAATGCTGATGATGCGCGGAGAGGTTGTGGCCGTGACGGGCGACGGGACGAAC  2250
720  A  R  S  Q  P  L  D  K  Q  L  L  V  L  M  L  M  M  R  G  E  V  V  A  V  T  G  D  G  T  N
     GATGCGCCCGCGCTACGACTGGCGAATGTTGGTTTTGTGATGCGGAGCGGGACGGACATTGCAGTGAAGTCGTCGGACATTGTGCTGCTG  2340
750  D  A  P  A  L  R  L  A  N  V  G  F  V  M  R  S  G  T  D  I  A  V  K  S  S  D  I  V  L  L
     GACGACAACTTCCGTTCCGTGCAGCGTGCCGTTGTGTGGGGGCGGACGGTCAACGACAACATTCGCAAGTTCTTGCAGCTGCAGCTGACT  2430
780  D  D  N  F  R  S  V  Q  R  A  V  V  W  G  R  T  V  N  D  N  I  R  K  F  L  Q  L  Q  L  T
     GTGAATGTTTCGAGCGTCGTACTGACGTTTCTCGGTTCGTTCTTGTCGTCCTCCCACACTTCCCCGCTGAGCACTGTGCAGCTGCTGTGG  2520
810  V  N  V  S  S  V  V  L  T  F  L  G  S  F  L  S  S  S  H  T  S  P  L  S  T  V  Q  L  L  W
     GTGAACCTGATAATGGACACGCTGGCTGCCCTTGCGCTCGCGACGGAGGAACCGTCGGAGGCGTGCCTGGACCGTGGCCCCATTCCCCGC  2610
840  V  N  L  I  M  D  T  L  A  A  L  A  L  A  T  E  E  P  S  E  A  C  L  D  R  G  P  I  P  R
     AAGGCCCCGCTTGTGTCACGCCGCATGTGGTGCACGATTCTTGCGATCGCTGGTTACCAAACCGTCAGCACACTATTGGTGGAACGATTT  2700
870  K  A  P  L  V  S  R  R  M  W  C  T  I  L  A  I  A  G  Y  Q  T  V  S  T  L  L  V  E  R  F
     GGCGGCTCGTGGTTTGATGTGAGTGGGGGTGAGATGCAGACTATAGTGTTTAATGTGTTTCTTCTTTCCGTTATTTTTCATATGTTCAAC  2790
900  G  G  S  W  F  D  V  S  G  G  E  M  Q  T  I  V  F  N  V  F  L  L  S  V  I  F  H  M  F  N
     GCACGCAAGTTGTACGAGGAGATGAATTGCTTCGAGGGGCTGTGGAAGCGCTCGAGAATTTTTGTTTGCATTGTTGGCTTTTGCTTTGCG  2880
930  A  R  K  L  Y  E  E  M  N  C  F  E  G  L  W  K  R  S  R  I  F  V  C  I  V  G  F  C  F  A
     TTCCAGGTGTTTTCCGTGGAGATGCTCGGGAGTTTTATGCAGGTTGTGTCGCTGCGCGGTGAGCAGTGGGTTGGTTGCCTGGCGTTGTCG  2970
960  F  Q  V  F  S  V  E  M  L  G  S  F  M  Q  V  V  S  L  R  G  E  Q  W  V  G  C  L  A  L  S
     TTCCTAACTCTTGTCTTTGGTGCGGTCGCGCGCTTGGTGCCTGTGGAGGAGCTACCGTTGCCGGAGGCGGAGATGGACGACATGGAGCCC  3060
990  F  L  T  L  V  F  G  A  V  A  R  L  V  P  V  E  E  L  P  L  P  E  A  E  M  D  D  M  E  P
     GAGGCGAGGCGCATGGCGATGAAGCTGACGGCTGATGTGGAGGCGCATGCGGCGAGGGAGGGCGCTGGTGGCCACCTGCTGCTGGGGCGG  3150
1020 E  A  R  R  M  A  M  K  L  T  A  D  V  E  A  H  A  A  R  E  G  A  G  G  H  L  L  L  G  R
     CGTCTGCTTGCCCAGGCCATGTGGCAGCAGGTGCGGGAGCACCACATCGCGGTGAGGAGCGTGAATGCCTTTCGGCGGGCCCGAATTGAT  3240
1050 R  L  L  A  Q  A  M  W  Q  Q  V  R  E  H  H  I  A  V  R  S  V  N  A  F  R  R  A  R  I  D
     CGTGACATGCACACAAGTGTTGCCAAAGACATTTATTGCCGCCTTGCATCCACCATGCAGTAACATACTTTGTGTGTGGGTGTGGGTGTG  3330
1080 R  D  M  H  T  S  V  A  K  D  I  Y  C  R  L  A  S  T  M  Q  *
     GCGAAGTATGCACTATGATACAATCGTTTTTTGATTATTATTTCAGAGATTGTTGCGAGGCGTGTGTTTTTACAGTCCACTCCAACCGAC
     CGAAATGCCGCGCGGGAGGTGGGTGAGGGGACGCCTTTGCACTGAGTATATATATATATATATACACGCCGCCATAAAAGCAAT
```

B

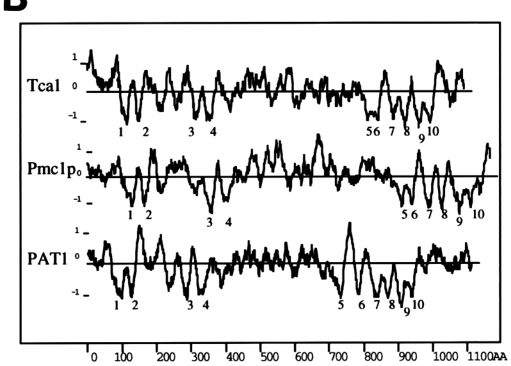

FIG. 1. (A) Nucleotide and predicted protein sequences of *tca1*. Amino acid residues are numbered in the left margin; nucleotides are numbered in the right margin. The amino acid sequences corresponding to the highly conserved catalytic autophosphorylation and ATP-binding domains employed in the design of degenerate oligodeoxyribonucleotides for PCR are in boldface. The 10 transmembrane domains identified by hydropathy analysis are underlined. The TAA stop codon for *tca1* is marked by an asterisk. Potential N-glycosylation sites are in boldface italics. (B) Hydropathy plots of *T. cruzi* Tca1, *S. cerevisiae* Pmc1p (9), and *D. discoideum* PAT1 (30). Putative transmembrane domains are numbered. Hydropathy was computed and putative transmembrane domains were predicted according to the method of Hopp and Woods (23) over a running window of 20 amino acid residues. Numbers at the bottom of the figure denote positions of the amino acid residues from the NH_2 terminus. Numbers on the ordinate are relative hydropathy values.

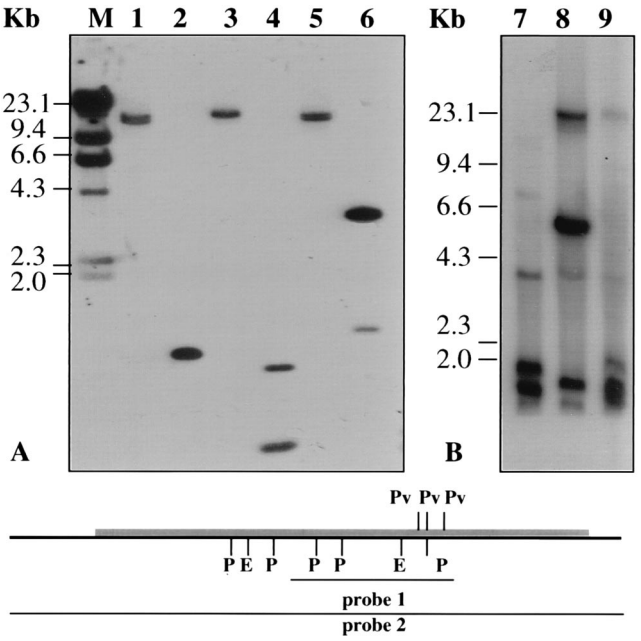

FIG. 2. Southern blot analysis of the *tca1* gene in genomic DNA from *T. cruzi*, *T. brucei*, *L. mexicana amazonensis*, and *L. donovani*. Total genomic DNA (10 μg/lane) was digested with various restriction enzymes and analyzed as described in Materials and Methods. Size markers (M) are indicated. (A) *T. cruzi* genomic DNA digested with the following restriction enzymes: lane 1, *Bam*HI; 2, *Eco*RI; 3, *Hin*dIII; 4, *Pst*I; 5, *Sac*I; 6, *Pvu*II. The blots were hybridized with the ^{32}P-labeled 1.0-kb PCR product (probe 1) and washed at high stringency. (B) Digestion with *Pst*I of 10 μg of genomic DNA from *T. brucei* (lane 7), *L. mexicana amazonensis* (lane 8), and *L. donovani* (lane 9). The blots were hybridized with the ^{32}P-labeled p*tca1* probe (probe 2) at 60°C and washed with 2× SSC at 60°C. The scheme shows the restriction sites in the *tca1* gene (gray area) and the probes used. P, *Pst*I; E, *Eco*RI; Pv, *Pvu*II.

with the vacuolar-type Ca^{2+}-ATPases described for *S. cerevisiae* and *D. discoideum*, respectively.

To obtain the complete gene, this PCR clone was used as a probe to screen a lambda EMBL3 genomic library of *T. cruzi*. Southern hybridization of *Bam*HI-digested genomic DNA with the 1.0-kb clone revealed a single ~20-kb hybridization band. Ten positive clones were obtained. Mapping and sequencing of these clones revealed a complete open reading frame (*tca1*) (Fig. 1A) with 3,300 nucleotides. The DNA sequence of the ~1.0-kb PCR product was identical to the corresponding region of the gene obtained from the lambda EMBL3 genomic library. According to the initiation codon ATG that was predicted (Fig. 1A), the open reading frame codes for a protein of 1,100 amino acids with a calculated molecular mass of 121,141 Da. Interestingly, about 150 to 300 bp upstream of the initiation codon, there are long stretches of adenines (Fig. 1A). These stretches are included in the *tca1* transcript, since the spliced leader addition sites were mapped to about 300 bp (minor site) and 450 bp (major site) upstream of the initiation codon (data not shown). Whether the adenine sequences are involved in the regulation of *tca1* expression is at present unknown.

Structure of the coding region and genomic organization of *tca1*. Analysis of the Tca1 amino acid sequence (Fig. 1A) showed that this gene product contains all the conserved subdomains and invariant residues found in other P-type ATPases, such as the phosphorylation and ATP-binding domains (1, 36). Hydropathy analysis (23) of the deduced amino acid sequence (Fig. 1B) revealed a profile very similar to those of other calcium pumps containing 10 transmembrane domains. As occurs with the vacuolar Ca^{2+}-ATPases described for *S. cerevisiae* (9) and *D. discoideum* (30), a TFASTA search of protein databases showed that Tca1 was closely related to the PMCA, with 38% identity (58% similarity) to the PMCA from human erythrocytes (53). It also had 34 and 38% identity and 56 and 59% similarity to the vacuolar Ca^{2+}-ATPases of *S. cerevisiae* (9) and *D. discoideum* (30), respectively, and had 23 to 27% identity with sarcoplasmic (endoplasmic) reticulum-type Ca^{2+}-ATPases (SERCA) and 20 to 25% identity with Na^+,K^+-ATPases from different species (29, 46). Tca1 contains four potential N-glycosylation sites (indicated in boldface italics in Fig. 1A).

Tca1 lacks the conserved amino acid sequence associated with calmodulin binding that is found near the C terminus of all mammalian PMCA isoforms (52), as is the case also for the vacuolar Ca^{2+}-ATPases from other lower eukaryotic organisms, such as Pmc1p of *S. cerevisiae* (9) and PAT1 of *D. discoideum* (30). Like PAT1 of *D. discoideum*, Tca1 also has a long extension, of about 100 amino acids, after transmembrane domain 10, which is absent in Pmc1p and which was used to generate specific antibodies (see below).

Genomic DNA was digested with several restriction enzymes (selected to demonstrate genome copy number) and hybridized at high stringency to the ~1.0-kb PCR product (Fig. 2A). There was strong hydridization between the PCR product (probe 1; see scheme in Fig. 2) and the genomic DNA of *T. cruzi*. Two bands were obtained when *Pst*I (lane 4) or *Pvu*II (lane 6) was used, in agreement with the presence of cleavage sites for these enzymes in the probe used (one additional band obtained with *Pst*I and two additional bands obtained with *Pvu*II were too small to be detected). *Eco*RI (lane 2) and *Hin*dIII (lane 3) produced single bands (Fig. 2A). Interestingly, although there is neither a *Bam*HI site nor a *Sac*II site in the coding region of *tca1*, treatment of DNA with these two restriction enzymes generated double hybridization bands of similar intensities and slightly different sizes. These double bands

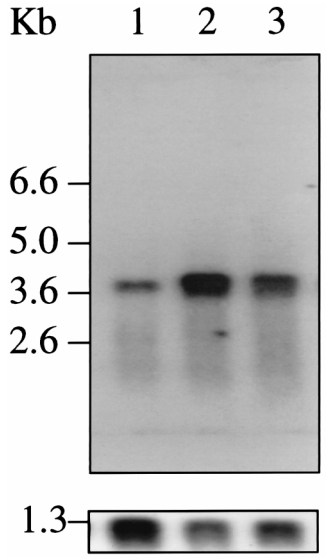

FIG. 3. Expression of *tca1* mRNA. (Upper panel) Poly(A)$^+$ RNAs isolated from epimastigotes (3 μg [lane 1]), amastigotes (1 μg [lane 2]), or trypomastigotes (3 μg [lane 3]) were electrophoresed, blotted, and probed at high stringency with the ^{32}P-labeled 1.0-kb PCR fragment. Size markers correspond to a 0.24- to 9.5-kb RNA ladder (Gibco BRL). Approximately equal amounts of RNA were observed in lanes 1 and 3 under UV light. (Lower panel) The membrane was stripped and reprobed with a ^{32}P-labeled PCR fragment of the *TcP0* gene from *T. cruzi* (47) as a control.

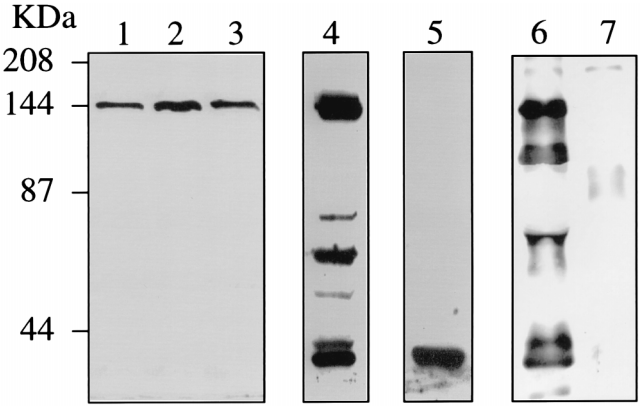

FIG. 4. Western blot analysis of Tca1. Homogenates containing 20 μg of protein from epimastigotes (lane 1), amastigotes (lane 2), and trypomastigotes (lane 3) were subjected to SDS-polyacrylamide gel electrophoresis on 7.5% polyacrylamide gels and transferred to nitrocellulose membranes. Lanes were probed with antibodies prepared as described in Materials and Methods. Lanes 4 and 5 show the proteolytic products obtained after incubation of epimastigote lysates in ice for 10 (lane 4) and 30 (lane 5) min in the absence of proteinase inhibitors. For lane 6, epimastigotes were incubated with biotin succinimidyl ester. After the cells were lysed, Ca^{2+}-ATPases were immunoprecipitated and the immunoprecipitate was subjected to Western blot analysis. Visualization of biotinylation was by streptavidin-peroxidase conjugate and ECL. Several bands were recognized. Lane 7 shows a control with normal serum instead of anti-Ca^{2+}-ATPase antibodies for immunoprecipitation. Migration positions of prestained molecular mass standards (Bio-Rad Laboratories, Hercules, Calif.) are shown to the left of the gels.

were more evident when long run gels (25 by 15 cm) were used (data not shown). The calculated sizes for the *Bam*HI (lane 1) and the *Sac*II (lane 5) double fragments were 14.0 and 14.5 kb and 15.0 and 15.5 kb, respectively. Taking into account the large size and similar intensities of hybridization and the same size difference obtained with different restriction enzymes, these bands are more likely coming from two alleles than from two copies of tandem repeats.

A *tca1*-related gene is also present in *T. brucei* (Fig. 2B, lane 7), *L. mexicana amazonensis* (Fig. 2B, lane 8), and *Leishmania donovani* (Fig. 2B, lane 9). Southern blots of genomic DNA from these trypanosomatids, hybridized with *tca1* (probe 2; see scheme in Fig. 2) at medium stringency (60°C, 2× SSC [1× SSC is 0.15 M NaCl plus 0.015 M sodium citrate]), revealed the presence of multiple cross-hybridizing bands. In this regard, a gene homologous to *tca1* has recently been cloned from *T. brucei* (27a).

Higher expression of *tca1* in intracellular forms of *T. cruzi*. Northern blot analysis showed a single ~4.3-kb transcript in each of the three life cycle stages of *T. cruzi* (Fig. 3, upper panel). Analysis of the ~4.3-kb band by densitometry indicated that the *tca1* transcript is >6-fold more abundant in amastigotes and >3-fold more abundant in trypomastigotes than in epimastigotes. Bands obtained after hybridization with a PCR product for the *TcP0* gene, which is expressed at similar levels in all stages of *T. cruzi* (47) (Fig. 3, lower panel), were used as a reference control.

To detect the *tca1* gene product, antibodies were raised against the C-terminal 174 amino acids of the protein fused to a six-histidine tag and purified as described in Materials and Methods. This region was chosen because it is the least conserved region of all known Ca^{2+}-ATPases: a C-terminal extension has been described before only for the vacuolar Ca^{2+}-ATPase from *D. discoideum* (30). Total homogenates prepared from different stages of *T. cruzi* were subjected to Western analysis with the affinity-purified antibodies. These antibodies detected a single band of approximately 140 kDa, close to the predicted molecular mass of Tca1 (Fig. 4, lanes 1 to 3). Membranes from amastigotes possessed at least a twofold-higher level of Tca1, as analyzed by densitometry (Fig. 4, lane 2), than did those from epimastigotes (Fig. 4, lane 1) or trypomastigotes (Fig. 4, lane 3). This elevated level of Tca1 was in agreement with the increased abundance of Tca1 message observed in amastigotes (Fig. 3). The protein was very susceptible to proteolysis (Fig. 4, lanes 4 and 5).

Functional complementation of the *PMC1* gene of *S. cerevisiae* with *tca1*. *S. cerevisiae* K665 with deletion of the genes encoding the high-affinity Ca^{2+}-ATPase and low-affinity Ca^{2+}/H^+ antiporter (*PMC1* and *VCX1*) is intolerant of high Ca^{2+} in the growth medium (10). Since the *T. cruzi tca1* gene encodes

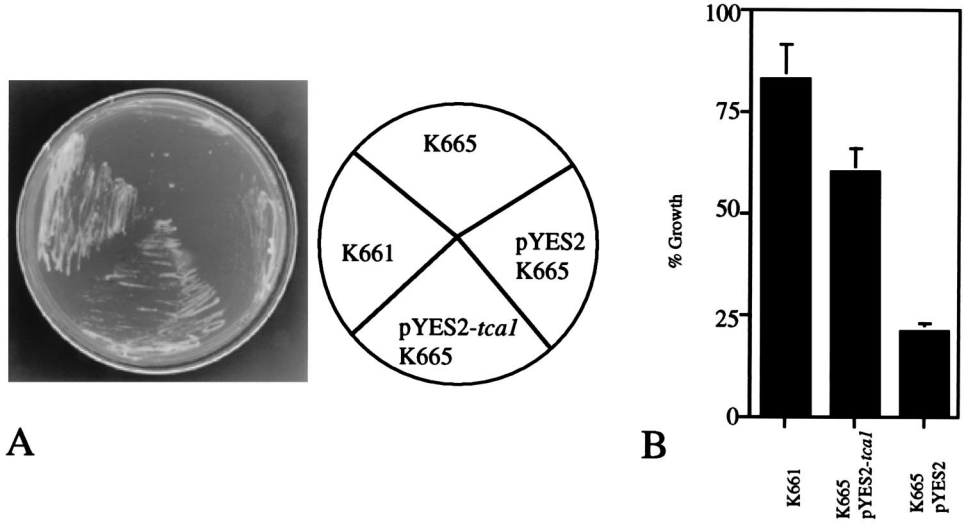

FIG. 5. Suppression of the Ca^{2+}-hypersensitivity of the *S. cerevisiae vcx1 pmc1* mutant by *T. cruzi tca1*. *S. cerevisiae vcx1 pmc1* strain K665 was transformed with a control vector (pYES2 K665) or a vector containing the entire open reading frame of *T. cruzi tca1* (pYES2-*tca1* K665). Strain K661 has the *PMC1* gene and thus served as the positive control. The cultures were streaked on YPD (1% Difco extract–2% Bacto Peptone–2% dextrose, pH 5.5) plates containing 200 mM $CaCl_2$ (A) or were inoculated into YPD (pH 5.5) with 200 mM $CaCl_2$, and growth was estimated by measuring the optical density at 600 nm (B), to identify Ca^{2+}-tolerant transformants.

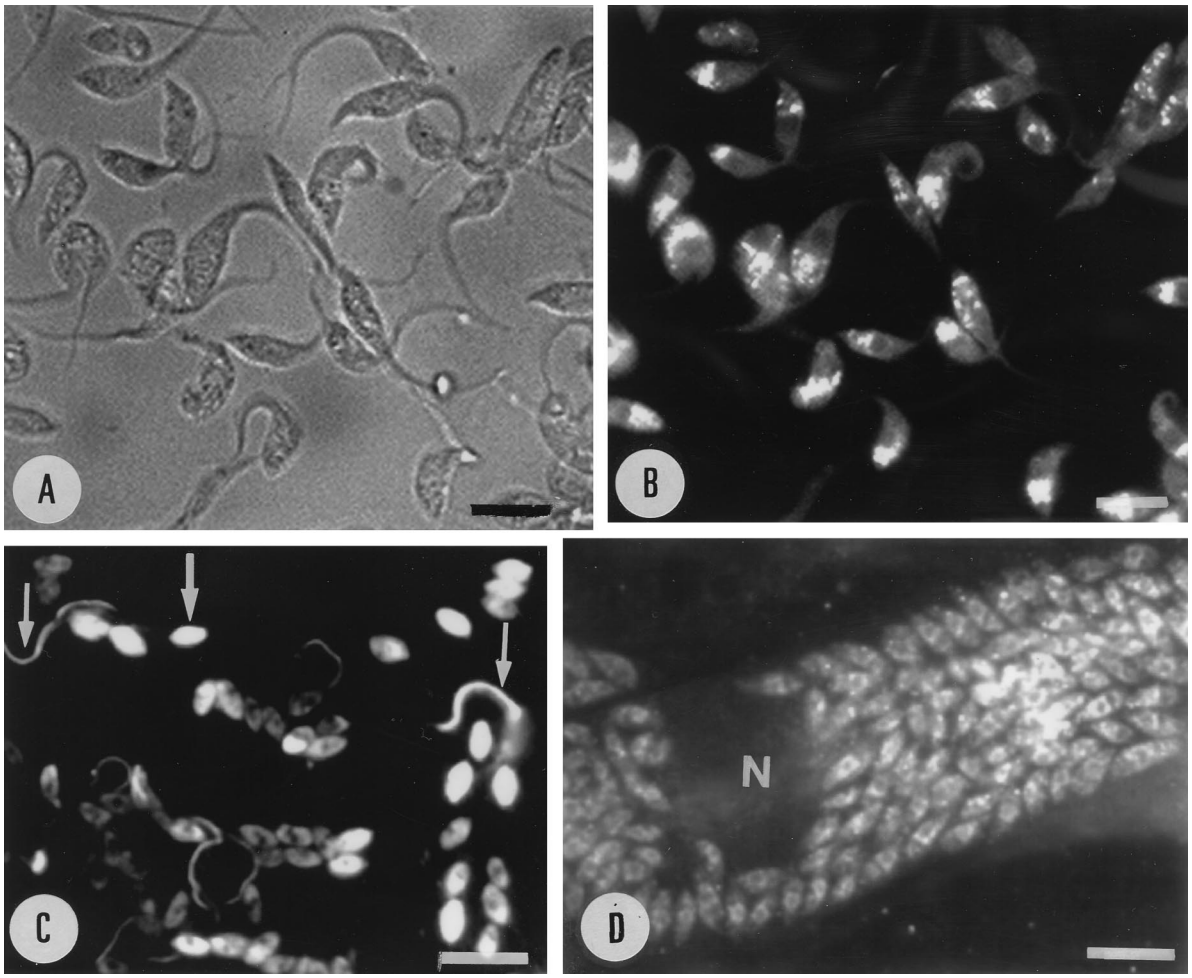

FIG. 6. Immunofluorescence microscopy showing the localization of Tca1 in epimastigote (B), trypomastigote (C), and extracellular (C) or intracellular (D) amastigote forms of *T. cruzi*. Panel A shows the same cells as in panel B by bright-field microscopy. Arrows indicate features discussed in the text. N, host cell nucleus. Bars, 20 μm.

a vacuolar-type Ca^{2+}-ATPase with homology to *PMC1*, we investigated whether complementation of the *vcx1 pmc1* yeast mutants with the *tca1* gene could suppress their Ca^{2+} hypersensitivity. Figure 5 shows that transformation of the *vcx1 pmc1* K665 strain with pYES2-*tca1* restored growth on high Ca^{2+} almost completely, thus suggesting the function of *tca1* as a vacuolar Ca^{2+}-ATPase in these mutants. K665 was transformed with a control vector (pYES2 K665) or a vector containing the entire open reading frame of *T. cruzi tca1* (pYES2-*tca1* K665). Strain K661 has the *PMC1* gene (10) and thus served as the positive control (Fig. 5).

Localization of *T. cruzi* Ca^{2+}-ATPase. We investigated the localization of the Ca^{2+}-ATPase in *T. cruzi* by immunocytochemistry with the antibodies described above. The reaction of these antibodies in the various developmental stages of *T. cruzi* as revealed with fluorescein-labeled secondary antibodies was of variable intensity. In epimastigotes, we observed labeling of cytoplasmic structures more frequently found in the posterior and central region and a weak labeling of the cell surface, including the flagellum (Fig. 6A and B). Live cells were not labeled with these antibodies (data not shown), in agreement with the cytoplasmic location of the C-terminal region of PMCA-type calcium pumps (7). Staining of the flagellum and the cell body was observed in trypomastigotes (Fig. 6C, thin arrows). Amastigotes were intensely stained when they were located either extracellularly (Fig. 6C, thick arrow) or intracellularly (Fig. 6D). This is in agreement with their higher calcium pump content (Fig. 4). No fluorescence was observed in control parasites incubated only in the presence of the secondary fluorescein-labeled goat anti-rabbit IgG (data not shown) or in the host cells (Fig. 6D).

To confirm the surface localization of the Ca^{2+}-ATPase in epimastiotes, we labeled these cells with biotin succinimidyl ester, a reagent that couples biotin to lysine residues of exposed proteins. The cells were incubated with the reagent and lysed, and the Ca^{2+}-ATPase was immunoprecipitated with the polyclonal antibody. The precipitated proteins were electrophoresed and blotted, and biotinylated proteins were visualized by peroxidase-conjugated streptavidin and ECL. Figure 4, lane 6, shows a 140-kDa polypeptide corresponding to the Ca^{2+}-ATPase and additional bands probably resulting from proteolysis of the 140-kDa polypeptide. The pattern of bands was very similar to that observed with epimastiote cell lysates incubated for 10 min in ice (Fig. 4, lane 4).

In order to analyze in more detail the structures labeled with the antibodies, immunoelectron microscopy was performed both on cryosections and on thin sections of parasites embedded in the Unicryl hydrophilic resin. The results obtained con-

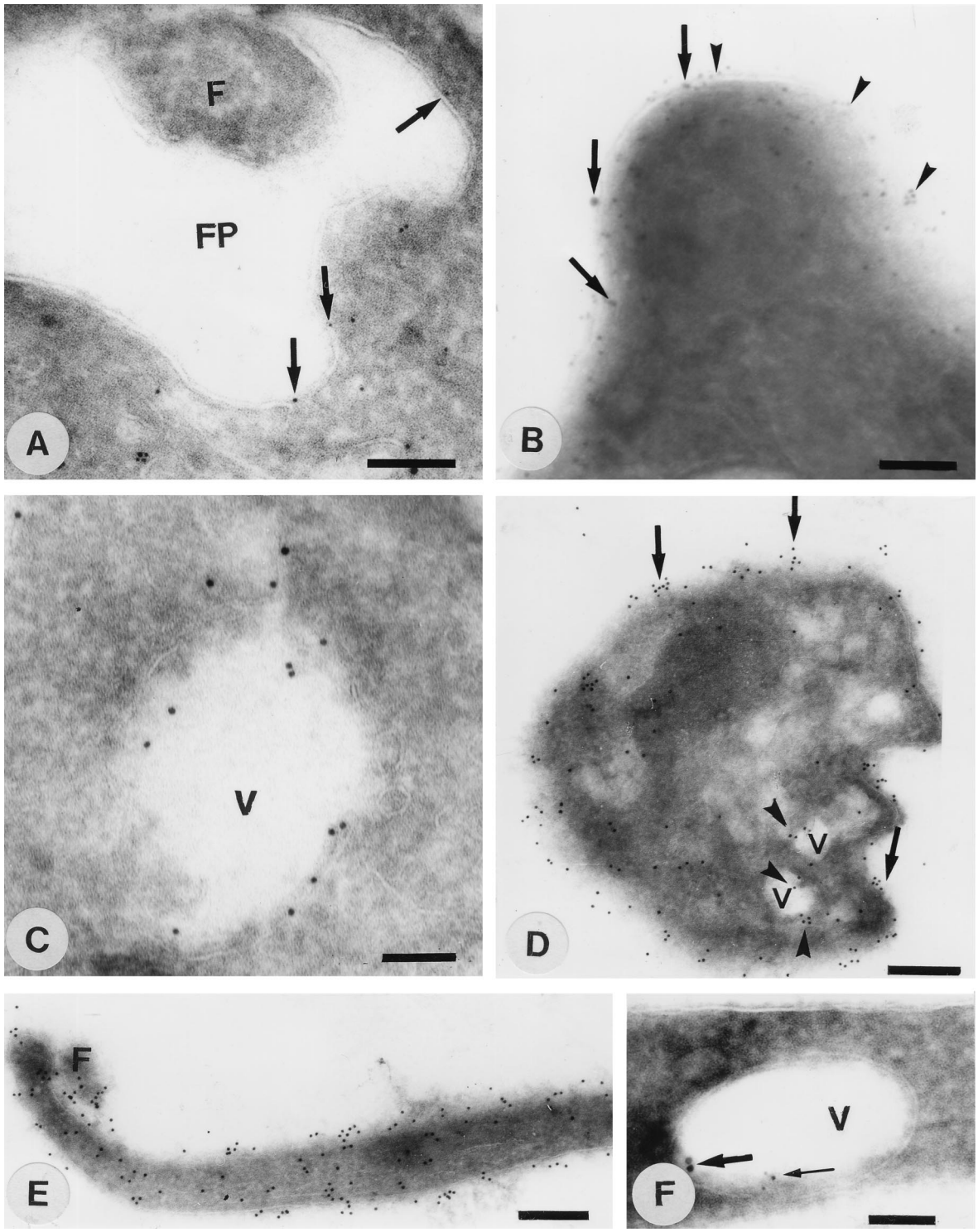

FIG. 7. Immunocytochemical localization of Ca^{2+}-ATPase (A to F) and H^+-ATPase (A, B, and F) in epimastigote (A, B, C, and F), amastigote (D), and trypomastigote (E) forms of *T. cruzi*. FP, flagellar pocket; F, flagellum; V, vacuole. Bars, 140 nm (A to C), 260 nm (D and E), and 100 nm (F). Note that 10-nm gold particles were used in panels B (thick arrows), C, and F (thick arrows) to localize the Ca^{2+}-ATPase while 5-nm particles were used in all other cases (A, D, and E). Conversely, 5-nm particles were used to localize the V-H^+-ATPase in panels B (arrowheads) and F (thin arrow), and 10-nm particles were used in panel A (no particles detected). Arrowheads in panel D show labeling of vacuoles, while arrows show surface labeling of amastigotes with antibodies against the Ca^{2+}-ATPase.

firmed that labeling intensity was higher in amastigotes, where gold particles were seen all over the protozoan surface (Fig. 7D, arrows) and in cytoplasmic vacuoles that appeared empty (arrowheads). In trypomastigotes, very few gold particles were observed in cytoplasmic structures (data not shown). However, labeling of the plasma membrane and the flagellum was observed (Fig. 7E), consistent with the results of immunofluorescence (Fig. 6C). In epimastigotes, labeling was observed both

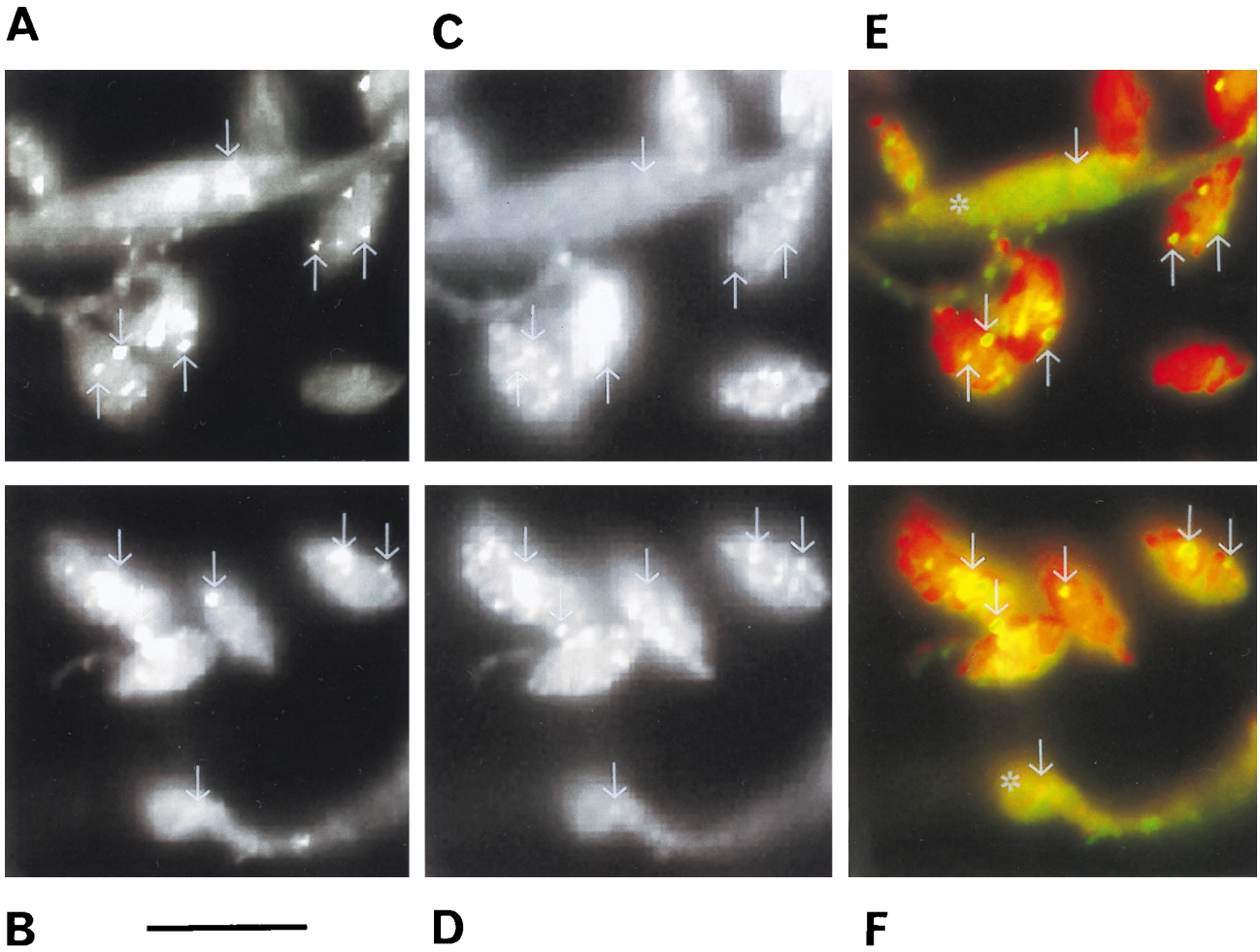

FIG. 8. Confocal laser scanning, microscopy showing the colocalization of V-H^+-ATPase (A and B; green in panels E and F) and Ca^{2+}-ATPase (C and D; red in panels E and F) in a mixture of amastigotes and epimastiotes (asterisks in panels E and F) of *T. cruzi*. Some of the vacuoles labeled with both antibodies are indicated with arrows in each picture and shown in yellow in panels E and F. Bar, 10 μm.

on the cell surface (Fig. 7B, arrows), including the portion lining the flagellar pocket (Fig. 7A, arrows), and in empty cytoplasmic vacuoles (Fig. 7C and F).

Colocalization studies were also done with the antibodies to the Ca^{2+}-ATPase (Fig. 8C and D) and a monoclonal antibody that recognizes the 110-kDa accessory protein of the V-H^+-ATPase (Fig. 8A and B) (18). This monoclonal antibody has been shown previously to cross-react with the V-H^+-ATPase of *L. mexicana* (54). Using confocal microscopy, we observed colocalization of the two ATPases both on the cell surface (Fig. 8A to D) and in cytoplasmic vacuoles (areas in yellow in Fig. 8E and F). The reaction of amastigotes with the antibodies against the Ca^{2+}-ATPase was stronger than that of epimastigotes in the same preparation (Fig. 8C and D). This is in agreement with a higher amount of calcium pump protein in amastigotes as shown in Fig. 4. Since we had to dilute these antibodies and decrease the exposure time in order to detect colocalization, a lower reaction was observed in epimastigotes as shown in Fig. 8C and D, compared to Fig. 6B. The reaction of both antibodies with two different membranes, the vacuolar and the plasma membrane, made difficult the detection of colocalization. However, it was clear that many vacuoles (see arrows) were labeled with both antibodies, and the superimposition of images obtained with the two antibodies resulted in the yellow vacuoles shown in Fig. 8E and F. Since there were areas in which colocalization was too weak or not apparent, we did colocalization studies using electron microscopy. The lack of colocalization in certain areas was confirmed by this method (Fig. 7A, B, and F). The Ca^{2+}-ATPase, but not the H^+-ATPase, was observed in the membrane lining the flagellar pocket (Fig. 7A), but both proteins were located in the plasma membrane (Fig. 7B) and in empty vacuoles (Fig. 7F). However, it is important to point out that in all experiments in which the two ATPases were localized in the same section, labeling density was very light, especially in the intracellular vacuoles (Fig. 7F). This could indicate a certain proximity of the antibody-binding sites of the two pumps. Functional studies have indicated that *T. cruzi* acidocalcisomes possess a V-H^+-ATPase and a Ca^{2+}-ATPase (14). Results here suggest that the empty vacuoles giving a positive reaction with both antibodies correspond to these organelles. Vacuoles positive with both antibodies were located close to the periphery of amastigotes (Fig. 7D and 8E and F), whereas in epimastigotes they occupied a more central and posterior region (Fig. 6B and 8E and F).

Localization of Ca^{2+}-containing vacuoles. In previous studies, we have indicated that most of the intracellular Ca^{2+} in different stages of *T. cruzi* is located in the acidocalcisomes

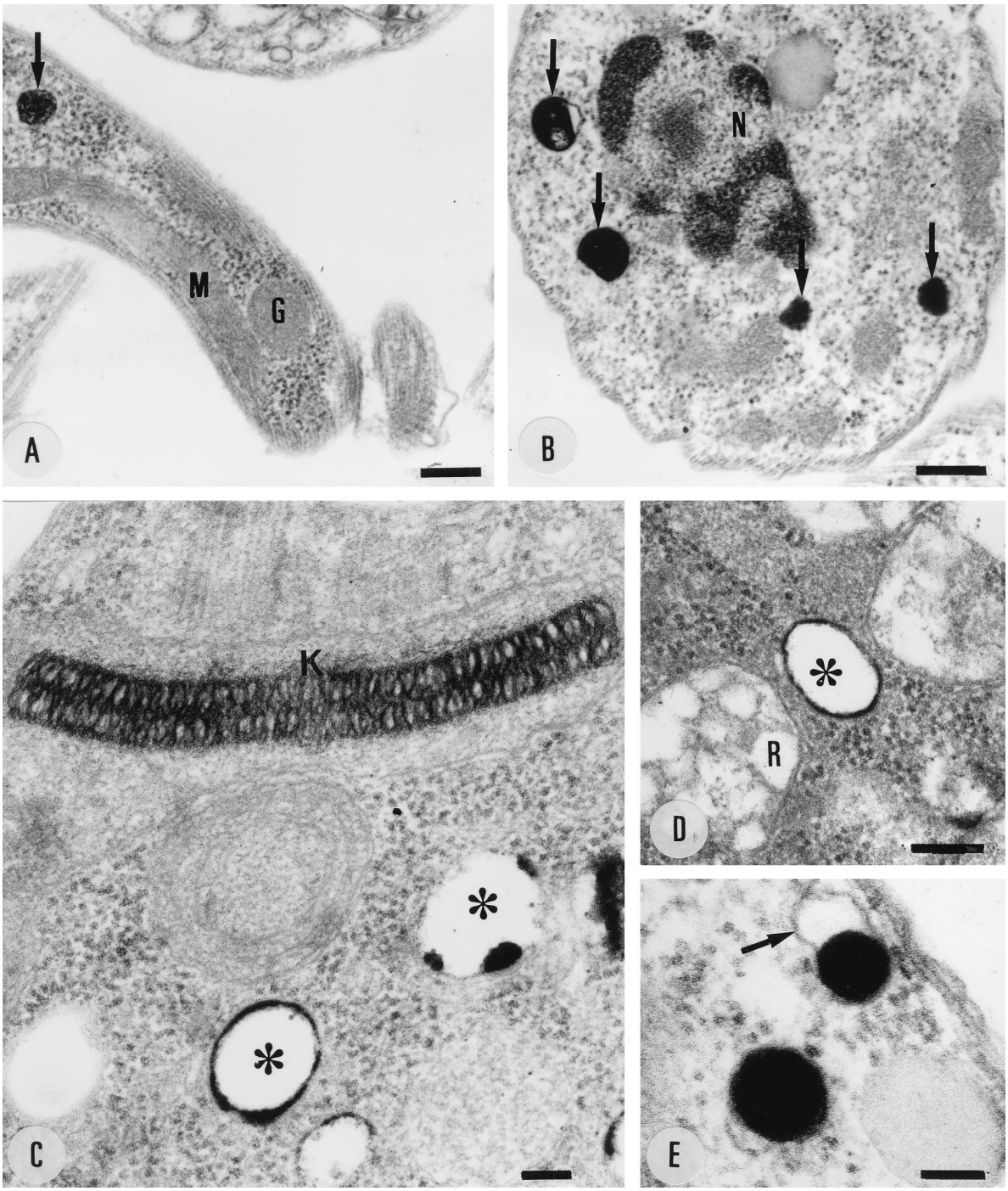

FIG. 9. Cytochemical localization of Ca^{2+} in trypomastigotes (A), amastigotes (B), and epimastigotes (C to E) incubated in the presence of potassium pyroantimoniate-osmium tetroxide solution. The electron-dense reaction product is restricted to cytoplasmic vacuoles (arrows in panels A and B and asterisks in panels C and D). The arrow in panel E shows the vacuole membrane. G, glycosome; K, kinetoplast; M, mitochondria; N, nucleus; R, reservosome. Bars, 250 (A), 200 (B), 80 (C), 170 (D), and 100 (E) nm.

(14). The use of quick-freezing, ultracryomicrotomy, and electron probe microanalysis to study the elemental composition of different compartments in *T. cruzi* epimastigotes with or without prior treatment with ionophores has recently provided evidence (44) that acidocalcisomes correspond to the electron-dense vacuoles previously described for these parasites (15). Because the vacuoles (presumptive acidocalcisomes) giving a reaction with antibodies against both ATPases appear empty and in some cases are irregular in shape in cryosections (Fig. 7C), we used a cytochemical technique to detect these organelles with better preservation of their structure than is possible with immunoelectron microscopy. In addition, it was important to establish the difference between these vacuoles and the lysosomal vacuoles present in epimastigotes known as reservosomes (48), which were also found to be acidic (49).

By the potassium pyroantimoniate-osmium technique, which

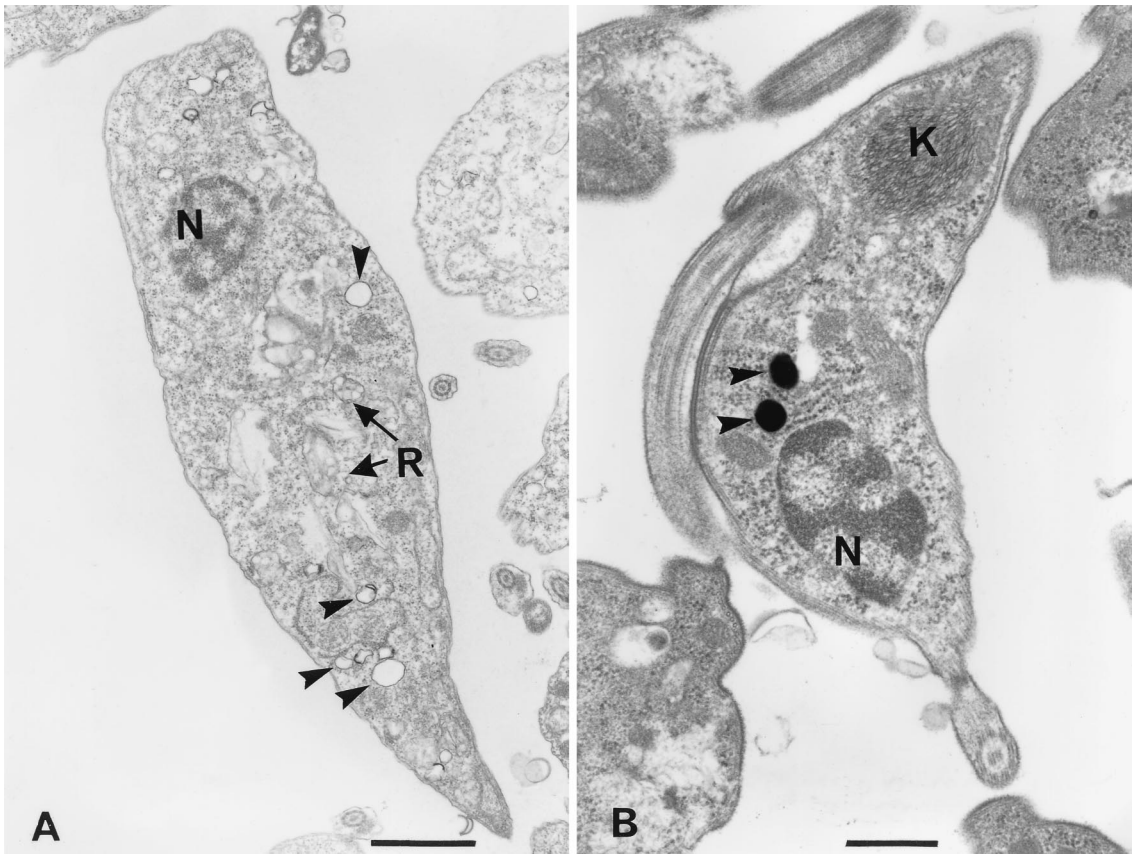

FIG. 10. Electron micrographs of control epimastigotes (A) and trypomastigotes (B). Cells were fixed as described in Materials and Methods. Arrowheads show empty vacuoles with an electron-dense material in their periphery in an epimastigote (A) and electron-dense vacuoles of similar size in a trypomastigote (B). N, nucleus; K, kinetoplast DNA; R, reservosomes. Bars, 1 μm (A) and 0.5 μm (B).

has been shown to localize Ca^{2+}-containing sites (3, 5, 64), a reaction product was observed in vacuoles of different stages of *T. cruzi* that were otherwise empty and surrounded by a typical membrane and had an average diameter of 210 ± 80 nm (± standard deviation [sd]) (Fig. 9), comparable with the diameter of the electron-dense vacuoles previously detected (44) in epimastigotes (200 ± 90 nm [± SD]). In most cases, the reaction product was restricted to the vacuolar periphery (Fig. 9C and D), but sometimes the reaction product occupied a large part of or even the whole vacuole (Fig. 9A, B, and E). The specificity of the technique was controlled by preventing formation of the reaction product with EGTA (data not shown), as described previously (5). Reaction product was not observed in other cytoplasmic structures, including the reservosomes (48, 49), which are abundant and occasionally located close to the calcium-containing vacuoles in epimastigote forms (Fig. 9D). Vacuoles similar in size to the calcium-containing vacuoles were identified in control preparations without pyroantimoniate (Fig. 10A). In most cases, these vacuoles appear empty but have a weakly electron-dense material in their periphery that makes their identification possible (Fig. 10A). In some cases, more notably in trypomastigotes, an electron-dense material occupies the whole vacuole (Fig. 10B). Similar vacuoles were observed in thin sections of amastigotes (data not shown). The correspondence of these vacuoles to the acidocalcisomes is indicated by several lines of evidence: (i) these vacuoles were the only ones to show a reaction by the potassium pyroantimoniate-osmium technique (Fig. 9), (ii) they had the same size and distribution as the electron-dense organelles detected in whole epimastiotes that were shown to be acidic and contain a high calcium concentration (44), and (iii) they had a similar appearance and distribution as the vacuoles containing the calcium and proton pumps (Fig. 6 to 8), as well as the vacuoles that take up acridine orange and by functional studies were identified as the acidocalcisomes (14).

In order to further distinguish acidocalcisomes from reservosomes, sections of Unicryl-embedded epimastiotes were incubated in the presence of antibodies recognizing cruzipain, a marker for reservosomes (51). The reservosomes were easily distinguished in thin sections stained with uranyl acetate and lead citrate, appearing as large spherical structures mainly located in the posterior region of epimastigotes (Fig. 11A). In sections incubated with anticruzipain antibodies, intense labeling of the cell surface and of large cytoplasmic vacuoles, which correspond to the reservosomes, was observed. However, vacuoles of similar size and appearance as the electron-dense vacuoles or acidocalcisomes were not labeled (Fig. 11B and C, asterisks). In contrast, when sections were incubated with anti-Ca^{2+}-ATPase antibodies, no labeling of reservosomes was observed (data not shown).

Detection of acidocalcisomes in whole parasites. We recently identified the electron-dense vacuoles present in epimastigotes as the acidocalcisomes (44), but similar experiments were not done with other cell types. Whole unfixed amastigotes and trypomastigotes were deposited on Formvar- and carbon-coated grids and examined by transmission electron microscopy. Electron-dense spherical structures appeared in large numbers in amastigotes (about 30 to 40 per cell [Fig. 12A and

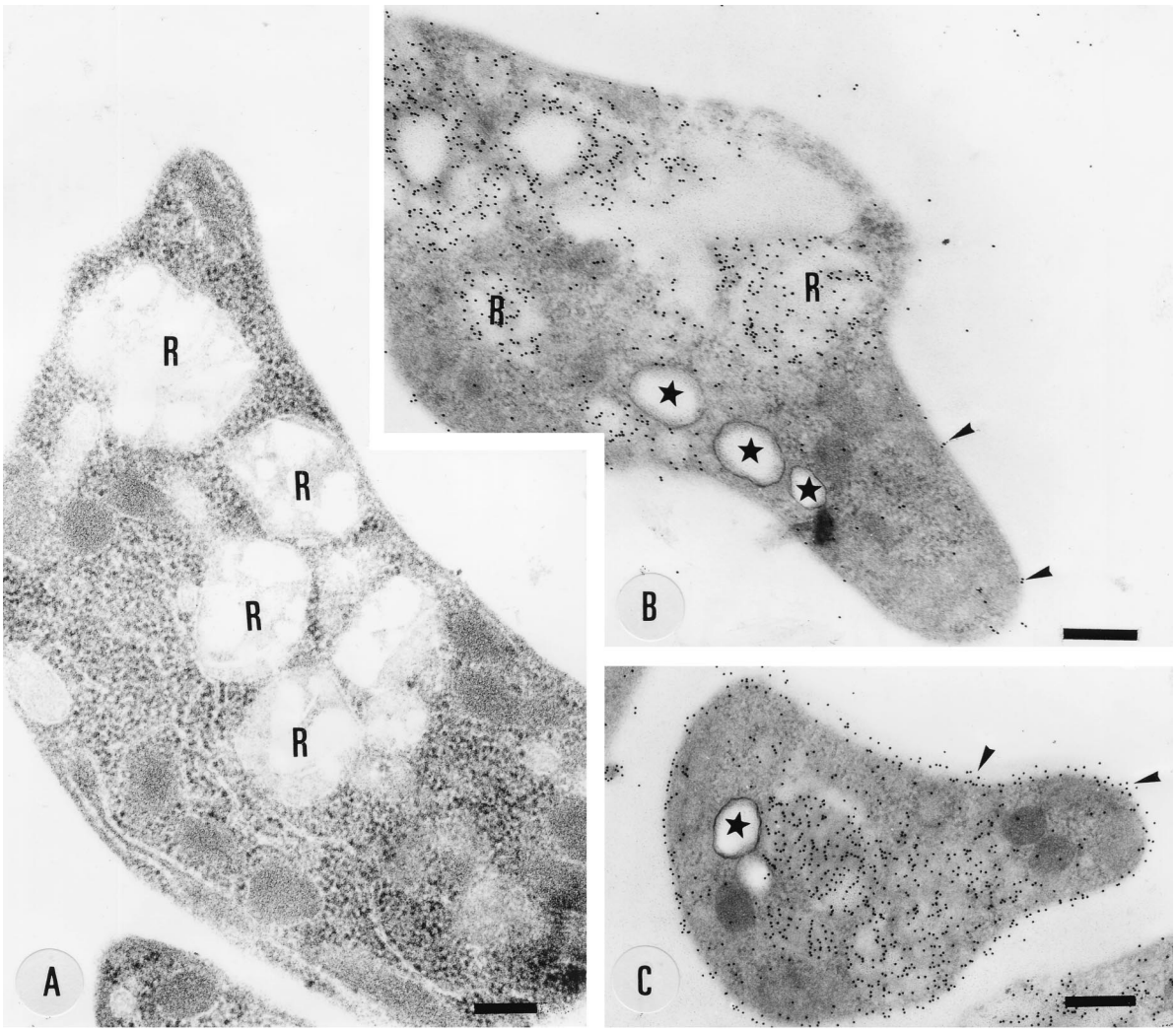

FIG. 11. Localization of cruzipain in thin sections of epimastigotes embedded in Unicryl. R, reservosomes. Arrowheads show labeling of the cell surface. Stars show the acidocalcisomes. Bars, 250 nm (A) and 330 nm (B and C).

B]) and in lower numbers in trypomastigotes (about 15 to 20 per cell [Fig. 12C and D]). In amastigotes, these vacuoles were occasionally arranged in rows and preferentially located towards the cell periphery, whereas in trypomastigotes they were located in the anterior region in close proximity to the flagellum. When they were submitted to the electron beam, we could observe changes in their internal structure leading to the appearance of a sponge-like structure (Fig. 12B).

Ca^{2+} content in different stages of *T. cruzi*. Because amastigotes express the vacuolar Ca^{2+}-ATPase to a greater extent (Fig. 4, 7D, and 8C and D) and have more electron-dense vacuoles or acidocalcisomes (Fig. 12) than the other stages, we investigated whether this was correlated with their intracellular Ca^{2+} content. Addition of 0.04% Triton X-100 to amastigotes (Fig. 13A), epimastigotes (Fig. 13B), or trypomastigotes (Fig. 13C) caused an immediate Ca^{2+} release. The total releasable Ca^{2+} of amastigotes (247 ± 20 nmol/mg of protein) was 6.2-fold higher than that of epimastigotes (40 ± 4 nmol/mg of protein) and 13.8-fold higher than that of trypomastigotes (19 ± 2 nmol/mg of protein) (mean ± SD from three different experiments).

DISCUSSION

In this work, we have shown that *T. cruzi* intracellular amastigotes possess a higher Ca^{2+} content than the extracellular stages of the parasite. This correlates firstly with the higher expression of a calcium pump, the gene for which was cloned and sequenced, and secondly with an abundance of acidocalcisomes or electron-dense vacuoles.

Comparison of the sequence of *tca1* from *T. cruzi* with other P-type ATPases indicates that this ATPase gene is closely related to the family of plasma membrane calcium (PMCA) pumps. The expression of *tca1* in a yeast mutant deficient in vacuolar Ca^{2+} accumulation (K665) provides genetic evidence that *tca1* encodes a vacuolar Ca^{2+} pump. This calcium pump was shown to be localized to intracellular vacuoles, and the plasma membrane of *T. cruzi*, as indicated by immunofluorescence (Fig. 6 and 8), immunoelectron microscopy (Fig. 7), and biotinylation experiments (Fig. 4). This pump apparently lacks the calmodulin-binding domain present in other PMCA pumps (52). This characteristic places this enzyme in a novel category together with the vacuolar Ca^{2+}-ATPases described for *S. cer-*

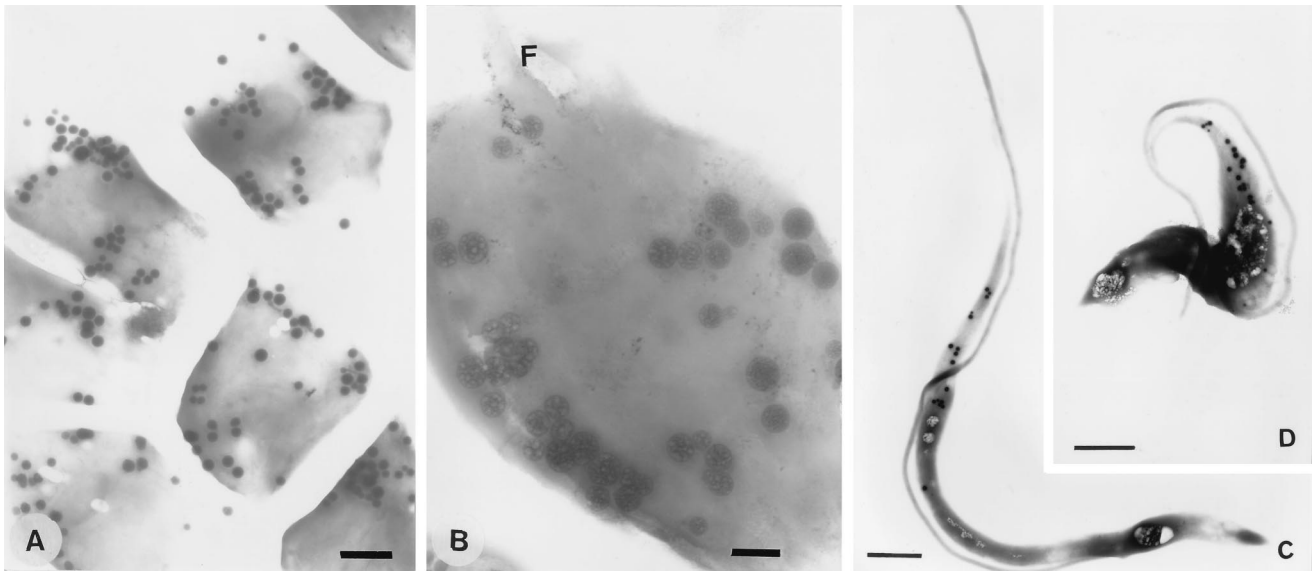

FIG. 12. Visualization of electron-dense vacuoles in whole unfixed amastigote and trypomastigote forms allowed to adhere to a Formvar- and carbon-coated grid and then observed in the transmission electron microscope. A large number of dense vacuoles can be seen in amastigotes, preferentially located towards the cell periphery (A and B), and a lower number can be seen in slender (C) and broad (D) trypomastigotes, preferentially located in the anterior region, close to the flagellum. F, flagellum. Bars, 1 μm (A, C, and D) and 0.3 μm (B).

evisiae (9) and *D. discoideum* (30). However, it is interesting to note that in a previous work (4) we were able to purify a plasma membrane-located Ca^{2+}-ATPase from *T. cruzi* epimastigotes by calmodulin affinity chromatography. The activity of the partially purified enzyme was stimulated by *T. cruzi* or bovine brain calmodulin. In addition, the enzyme cross-reacted with antiserum and monoclonal (5F10) antibodies raised against human erythrocyte Ca^{2+}-ATPase, had a molecular mass of 140 kDa, and formed Ca^{2+}-dependent hydroxylamine-sensitive phosphorylated intermediates (4). These results could indicate either the presence of two Ca^{2+}-ATPases in the plasma membrane of these parasites, perhaps with different activities in different stages, or the existence of a calmodulin-binding domain different from that previously identified in other plasma membrane Ca^{2+}-ATPases (53). As in the case of *D. discoideum* PAT1 (30), we cannot rule out the possibility that calmodulin regulates Tca1 activity by interacting with as-yet-unidentified sequences on the enzyme. Alternatively, Tca1 could be present in the plasma membrane of epimastigotes due to normal membrane recycling or targeting mechanisms. In addition, the strong reactivity of the antibody against Tca1 in the flagellar region of trypomastigotes (Fig. 6C and 7E) could suggest a different role for this pump in this stage of the parasite.

The identification of the intracellular vacuoles labeled with antibodies to the calcium pump as acidocalcisomes is suggested by the following lines of evidence. Prior biochemical data has indicated that acidocalcisomes are acidified by a vacuolar-type proton-translocating V-H^+-ATPase, that they possess a Ca^{2+}/H^+ countertransporting ATPase for Ca^{2+} uptake, and that they contain most of the parasite's intracellular Ca^{2+} (14). In this work, we show that calcium and proton pumps colocalize to intracellular vacuoles (Fig. 7 and 8). These vacuoles have the same cellular distribution as and are morphologically indistinguishable from the vacuoles that give a strong reaction with potassium pyroantimoniate in combination with osmium (Fig. 9), a method that has been widely used for the localization of calcium in different cells (3, 5, 64). In addition, they have the same cellular distribution as and are similar in size to the electron-dense vacuoles that we previously demonstrated are the acidocalcisomes (44). In conventional thin sections, these intracellular vacuoles may appear empty or may contain more or less electron-dense material (Fig. 10). Observation of whole unfixed parasites by transmission electron microscopy (Fig. 12) showed that these electron-dense vacuoles have a uniform inner structural organization that changes following exposure to the electron beam, as previously reported for isolated sarcoplasmic reticulum vesicles loaded with calcium phosphate or oxalate (11).

We also provided evidence that acidocalcisomes are distinct from other organelles previously recognized in these parasites. In contrast to the appearance of the acidocalcisomes, the ly-

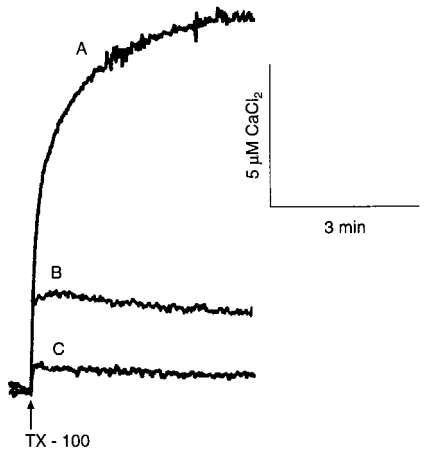

FIG. 13. Endogenous Ca^{2+} release from Triton X-100-permeabilized cells. Triton X-100 (TX-100; 0.04%) was added where indicated by the arrow to *T. cruzi* amastigotes 55 μg of protein/ml [A]), epimastigotes (90 μg of protein/ml [B]), or trypomastigotes (60 μg of protein/ml [C]) in a buffer containing 130 mM KCl, 1 mM $MgCl_2$, 2 mM K_2HPO4, 20 mM Tris-HCl (pH 7.4), and 40 μM arsenazo III at 30°C. Results shown are from representative experiments.

sosomal compartment known as the reservosome, present only in *T. cruzi* epimastigotes, contains intravacuolar inclusions (48, 49). Reservosomes were not labeled with antibodies against the Ca^{2+}-ATPase (data not shown) or by the potassium pyroantimoniate-osmium technique (Fig. 9). Furthermore, the morphology of the electron-dense vacuoles (acidocalcisomes) is clearly different from that of typical lysosomes (27). This evidence is also supported by previous subcellular fractionation and gold-labeled transferrin studies of *T. cruzi* epimastigotes which provided evidence that acidocalcisomes are different from lysosomes, endosomes, and reservosomes (44).

Dvorak et al. (15) first reported the presence of calcium-rich organelles in *T. cruzi* epimastigotes following energy-dispersive X-ray microanalysis. These cells were shown to possess electron-dense vacuoles identified by scanning transmission electron microscopy of whole cells. These vacuoles contain large amounts of magnesium, potassium, calcium, phosphorus, and zinc (15) and are morphologically indistinguishable from the electron-dense vacuoles that we detected in unfixed amastigotes and trypomastigotes (Fig. 12). Similar calcium-containing electron-dense vacuoles have also been described for other trypanosomatids such as *Trypanosoma cyclops* (60), *Trypanosoma rhodesiense* (65), and *Leishmania major* (26) and were named polyphosphate (60) or electron-dense (26, 60) vacuoles. These vacuoles were examined by energy-dispersive X-ray microanalysis (26, 60, 65) and in some cases were also observed by scanning transmission electron microscopy of whole cells (26), as were the electron-dense organelles found in *T. cruzi* (15). Acidocalcisomes have been found in all trypanosomatids examined to date (14, 28, 43, 58, 59), which further supports the suggestion that they correspond to the electron-dense vacuoles described for all these parasites.

The concentration of Ca^{2+} in the cytosol of vertebrate cells is known to be about 0.1 μM, which is dramatically different from the concentration of Ca^{2+} to which extracellular parasites are exposed (about 1 mM). The higher amount of Ca^{2+} in amastigotes would appear to indicate an adaptation to an intracellular environment. In this regard, we have shown previously that amastigotes of *L. mexicana amazonensis* also possess a higher amount of releasable Ca^{2+} and exhibit greater expression of a SERCA-type Ca^{2+}-ATPase than do the extracellular promastigotes (28). Although SERCA-type Ca^{2+}-ATPases are usually located in the endoplasmic (sarcoplasmic) reticulum, some SERCA-type Ca^{2+}-ATPases have been shown elsewhere to be localized to plant vacuoles (17). It is possible either that a SERCA-type Ca^{2+}-ATPase replaces a Tca1 homolog in *Leishmania* or that both calcium pumps are highly expressed in intracellular forms of these parasites, thus explaining their higher calcium content.

It has been demonstrated that the Ca^{2+} content of intracellular stores exerts a profound control over cell growth and the progression of cells through the cell cycle and that growth changes can result from the inability of Ca^{2+} to be pumped into intracellular stores (45). Our results provide further support for the link between intracellular Ca^{2+} pool content, expression of Ca^{2+}-ATPases, Ca^{2+} signaling, cell growth in eukaryotic cells (45, 63), parasite virulence (28), and intracellular adaptation.

ACKNOWLEDGMENTS

We thank Richard Crang for help with the electron micrographs of whole trypomastigotes, Juan Jose Cazzulo for his generous gift of antibodies, Kyle W. Cunningham for generously providing yeast strains, David A. Scott for critically reading the manuscript, Lois L. Hoyer for useful discussions, Lou Ann Miller for help in processing material for electron microscopy, and Tetsuya Furuya for the *TcP0* probe.

This work was supported by grants from the National Institutes of Health (AI-23259 and TW00476) to R.D. and S.M. M.B. and W.D. were supported by grants from the Programa de Nucleos de Excelencia (PRONEX), the Financiadora de Estudos e Projetos (FINEP), and the Conselho Nacional de Desenvolvimento Científico e Tecnológico (CNPq), Brazil.

REFERENCES

1. **Allen, G., and N. M. Green.** 1976. A 31-residue tryptic peptide from the active site of the [Ca^{++}]-transporting adenosine triphosphatase of rabbit sarcoplasmic reticulum. FEBS Lett. **63:**188–192.
2. **Antebi, A., and G. R. Fink.** 1992. The yeast Ca^{2+} ATPase homologue, PMR1, is required for normal Golgi function and localizes in a novel Golgi-like distribution. Mol. Biol. Cell. **3:**633–654.
3. **Appleton, J., and D. C. Morris.** 1979. The use of potassium pyroantimoniate-osmium method as a means of identifying and localizing calcium at the ultrastructural level in the cells of calcifying systems. J. Histochem. Cytochem. **27:**676–680.
4. **Benaim, G., S. N. J. Moreno, G. Hutchinson, V. Cerviño, T. Hermoso, P. J. Romero, F. Ruiz, W. de Souza, and R. Docampo.** 1995. Characterization of the plasma membrane calcium pump from *Trypanosoma cruzi*. Biochem. J. **306:**299–303.
5. **Benchimol, M., C. A. Elias, and W. de Souza.** 1982. *Tritrichomonas foetus*: ultrastructural localization of calcium in the plasma membrane and in the hydrogenosomes. Exp. Parasitol. **54:**277–284.
6. **Blackford, S. B., P. A. Rea, and D. Sanders.** 1990. Voltage sensitivity of H^+/Ca^{2+} antiport in higher plant tonoplast suggests a role in vacuolar calcium accumulation. J. Biol. Chem. **265:**9617–9620.
7. **Carafoli, E.** 1991. Calcium pump of the plasma membrane. Physiol. Rev. **71:** 129–153.
8. **Clapham, D. E.** 1995. Calcium signaling. Cell **80:**259–268.
9. **Cunningham, K. W., and G. R. Fink.** 1994. Calcineurin-dependent growth control in *Saccharomyces cerevisiae* mutants lacking *PMC1*, a homolog of plasma membrane Ca^{2+} ATPases. J. Cell Biol. **124:**351–363.
10. **Cunningham, K. W., and G. R. Fink.** 1996. Calcineurin inhibits *VCX1*-dependent H^+/Ca^{2+} exchange and induces Ca^{2+} ATPases in *Saccharomyces cerevisiae*. Mol. Cell. Biol. **16:**2226–2237.
11. **de Meis, L., W. Hasselbach, and R. D. Machado.** 1974. Characterization of calcium oxalate and calcium phosphate deposits in sarcoplasmic reticulum vesicles. J. Cell Biol. **62:**505–509.
12. **de Souza, W.** 1984. Cell biology of *Trypanosoma cruzi*. Int. Rev. Cytol. **86:** 197–283.
13. **Docampo, R., and S. N. J. Moreno.** 1996. The role of Ca^{2+} in the process of cell invasion by intracellular parasites. Parasitol. Today **12:**61–65.
14. **Docampo, R., D. A. Scott, A. E. Vercesi, and S. N. J. Moreno.** 1995. Intracellular Ca^{2+} storage in acidocalcisomes of *Trypanosoma cruzi*. Biochem. J. **310:**1005–1012.
15. **Dvorak, J. A., J. C. Engel, R. D. Leapman, C. R. Swyt, and P. A. Pella.** 1988. *Trypanosoma cruzi*: elemental composition heterogeneity of cloned stocks. Mol. Biochem. Parasitol. **31:**19–26.
16. **Ezaki, J., M. Himeno, and K. Kato.** 1992. Purification and characterization of (Ca^{2+}-Mg^{2+})ATPase in rat liver lysosomal membranes. J. Biochem. (Tokyo) **282:**33–39.
17. **Ferrol, N., and A. B. Bennett.** 1996. A single gene may encode differentially localized Ca^{2+}-ATPases in tomato. Plant Cell **8:**1159–1169.
18. **Fok, A. K., M. Clarke, L. Ma, and R. D. Allen.** 1993. Vacuolar H($^+$)-ATPase of *Dictyostelium discoideum*. A monoclonal antibody study. J. Cell Sci. **106:** 1103–1113.
19. **Gerasimenko, O. V., J. V. Gerasimenko, P. V. Belan, and O. H. Petersen.** 1996. Inositol trisphosphate and cyclic ADP-ribose-mediated release of Ca^{2+} from single isolated pancreatic zymogen granules. Cell **84:**473–480.
20. **Gornall, A. G., C. J. Bardawill, and M. M. David.** 1949. Determination of serum proteins by means of the biuret reaction. J. Biol. Chem. **177:**751–766.
21. **Gunteski-Hamblin, A. M., D. M. Clarke, and G. E. Shull.** 1992. Molecular cloning and tissue distribution of alternatively spliced mRNAs encoding possible mammalian homologues of the yeast secretory pathway calcium pump. Biochemistry **31:**7600–7608.
22. **Hart, L. M. T., D. Lindhout, G. C. M. Van der Zon, H. Kayseilli, M. Y. Apak, W. J. Kleijer, E. R. Van der Vorm, and J. A. Massen.** 1996. An insulin receptor mutant (Asp^{707}-Ala), involved in leprechaunism, is processed and transported to the cell surface but unable to bind insulin. J. Biol. Chem. **271:** 18719–18724.
23. **Hopp, T. P., and K. R. Woods.** 1981. Prediction of protein antigenic determinants from amino acid sequences. Proc. Natl. Acad. Sci. USA **78:**3824–3828.
24. **Komnick, H., and U. Komnick.** 1963. Electronen-mikroskopische untersuchungen zur funktionellen morphologie des tonentransporters in der Salzdruse von *Lurus argentarus*. V. Experimenteller Nachweis der Transporwege. Z. Zellforsch. Mikrosk. Anat. **60:**163–172.

25. **Laemmli, U. K.** 1970. Cleavage of structural proteins during the assembly of the head of bacteriophage T4. Nature **227:**680–685.
26. **LeFurgey, A., P. Ingram, and J. J. Blum.** 1990. Elemental composition of polyphosphate-containing vacuoles and cytoplasm of *Leishmania major*. Mol. Biochem. Parasitol. **40:**77–86.
27. **Leighton, F., B. Poole, H. Beaufay, P. Baudhuin, J. W. Coffey, S. Fowler, and C. de Duve.** 1968. The large-scale separation of peroxisomes, mitochondria and lysosomes from the livers of rats injected with Triton WR-1339. J. Cell Biol. **37:**482–513.

27a. **Lu, H.-G., and R. Docampo.** Unpublished results.

28. **Lu, H.-G., L. Zhong, K. P. Chang, and R. Docampo.** 1997. Intracellular Ca^{2+} pool content and signaling, and expression of a calcium pump are linked to virulence in *Leishmania mexicana amazonensis*. J. Biol. Chem. **272:**9464–9473.
29. **Monastyrskaya, G. S., N. E. Broude, A. M. Melkov, Y. V. Smirnov, I. V. Malyshev, S. G. Arsenyan, I. S. Salomatina, V. E. Sverdlov, A. V. Grishin, K. E. Petrukhin, and N. N. Modyanov.** 1987. The primary structure of the alpha-subunit of Na^+, K^+-ATPase. III. The complete nucleotide sequence corresponding to the coding part of the gene. Bioorg. Khim. **13:**20–26.
30. **Moniakis, J., M. B. Coukell, and A. Forer.** 1995. Molecular cloning of an intracellular P-type ATPase from *Dictyostelium* that is up-regulated in calcium-adapted cells. J. Biol. Chem. **270:**28276–28281.
31. **Moreno, S. N. J., J. Silva, A. E. Vercesi, and R. Docampo.** 1994. Cytosolic free calcium elevation in *Trypanosoma cruzi* is required for cell invasion. J. Exp. Med. **180:**1535–1540.
32. **Moreno, S. N. J., and L. Zhong.** 1996. Acidocalcisomes in *Toxoplasma gondii* tachyzoites. Biochem. J. **313:**655–659.
33. **Nadal-Ginard, B.** 1978. Commitment, fusion and biochemical differentiation of a myogenic cell line in the absence of DNA synthesis. Cell **15:**855–864.
34. **Ohsumi, Y., and Y. Anraku.** 1983. Calcium transport driven by a proton motive force in vacuolar membrane vesicles of *Saccharomyces cerevisiae*. J. Biol. Chem. **258:**5614–5617.
35. **Ortega-Barria, E., and M. E. A. Pereira.** 1992. Entry of *Trypanosoma cruzi* into eukaryotic cells. Infect. Agents Dis. **1:**136–140.
36. **Pick, U., and S. Bassilian.** 1981. Modification of the ATP binding site of the Ca^{2+}-ATPase from sarcoplasmic reticulum by fluorescein isothiocyanate. FEBS Lett. **123:**127–130.
37. **Pozzan, T., R. Rizzuto, P. Volpe, and J. Meldolesi.** 1994. Molecular and cellular physiology of intracellular calcium stores. Physiol. Rev. **74:**595–636.
38. **Rudolph, H. K., A. Antebi, G. R. Fink, C. M. Buckley, T. E. Dorman, J. Levitre, L. S. Davidow, I. Mao, and D. T. Moir.** 1989. The yeast secretory pathway is perturbed by mutation in *PMR1*, a member of a Ca^{2+}-ATPase family. Cell **58:**133–145.
39. **Sambrook, J., E. F. Fritsch, and T. Maniatis.** 1989. Molecular cloning: a laboratory manual, 2nd ed. Cold Spring Harbor Laboratory Press, Cold Spring Harbor, N.Y.
40. **Sanger, F., S. Nicklen, and A. R. Coulson.** 1977. DNA sequencing with chain-terminating inhibitors. Proc. Natl. Acad. Sci. USA **74:**5463–5467.
41. **Scala, C., G. Cenacchi, C. Ferrari, G. Pasquinelli, P. Preda, and G. C. Manara.** 1992. A new acrylic resin formulation: a useful tool for histologic, ultrastructural and immunocytochemical investigations. J. Histochem. Cytochem. **40:**1799–1804.
42. **Schmatz, D. M., and P. K. Murray.** 1982. Cultivation of *Trypanosoma cruzi* in irradiated muscle cells: improved synchronization and enhanced trypomastigote production. Parasitology **85:**115–125.
43. **Scott, D. A., S. N. J. Moreno, and R. Docampo.** 1995. Ca^{2+} storage in *Trypanosoma brucei*: the influence of cytoplasmic pH and importance of vacuolar acidity. Biochem. J. **310:**780–794.
44. **Scott, D. A., R. Docampo, J. A. Dvorak, S. Shi, and R. D. Leapman.** 1997. In situ compositional analysis of acidocalcisomes in *Trypanosoma cruzi*. J. Biol. Chem. **272:**28020–28029.
45. **Short, A. D., J. Bian, T. K. Ghosh, R. T. Waldrom, S. L. Rybak, and D. L. Gill.** 1993. Intracellular Ca^{2+} pool content is linked to control of cell growth. Proc. Natl. Acad. Sci. USA **90:**4986–4990.
46. **Shull, G. E., J. Greeb, and J. B. Lingrel.** 1986. Molecular cloning of three distinct forms of the Na^+,K^+-ATPase alpha-subunit from rat brain. Biochemistry **25:**8125–8132.
47. **Skeiky, Y. A. W., D. R. Benson, M. Parsons, K. B. Elkon, and S. G. Reed.** 1992. Cloning and expression of *Trypanosoma cruzi* ribosomal protein P0 and epitope analysis of anti-P0 autoantibodies in Chagas' disease patients. J. Exp. Med. **176:**201–211.
48. **Soares, M. J., and W. de Souza.** 1991. Endocytosis of gold-labeled proteins and LDL by *Trypanosoma cruzi*. Parasitol. Res. **77:**461–469.
49. **Soares, M. J., T. Souto-Padron, and W. de Souza.** 1992. Identification of a large prelysosomal compartment in the pathogenic protozoon *Trypanosoma cruzi*. J. Cell Sci. **102:**157–167.
50. **Somlyo, A. V., R. Broderick, H. Shuman, E. L. Buhle, and A. P. Somlyo.** 1988. Atrial-specific granules in situ have high calcium content, are acidic, and maintain anion gradients. Proc. Natl. Acad. Sci. USA **85:**6222–6226.
51. **Souto-Padron, T., O. E. Campetella, J. J. Cazzulo, and W. de Souza.** 1990. Cysteine proteinase in *Trypanosoma cruzi*: immunocytochemical localization and involvement in parasite-host cell interaction. J. Cell Sci. **96:**485–490.
52. **Strehler, E. E.** 1991. Recent advances in the molecular characterization of plasma membrane Ca^{2+} pumps. J. Membr. Biol. **120:**1–15.
53. **Strehler, E. E., P. James, R. Fischer, R. Heim, T. Vorherr, A. G. Filoteo, J. T. Penniston, and E. Carafoli.** 1990. Peptide sequence analysis and molecular cloning reveal two calcium pump isoforms in the human erythrocyte membrane. J. Biol. Chem. **265:**2835–2842.
54. **Sturgill-Koczycki, S., P. H. Schlesinger, P. Chakraborty, P. L. Haddix, H. L. Collins, A. K. Fok, R. D. Allen, S. L. Gluck, J. Heuser, and D. G. Russell.** 1994. Lack of acidification in *Mycobacterium* phagosomes produced by exclusion of the vesicular proton-ATPase. Science (Washington, D.C.) **263:**678–681.
55. **Tokuyasu, K. T.** 1989. Use of poly(vinylpyrrolidone) and poly(vinyl alcohol) for cryoultramicrotomy. Histochem. J. **21:**163–171.
56. **Towbin, H., T. Staehelin, and J. Gordon.** 1979. Electrophoretic transfer of proteins from polyacrylamide gels to nitrocellulose sheets: procedure and some applications. Proc. Natl. Acad. Sci. USA **76:**4350–4354.
57. **Ule, D. I., S. A. Ernst, H. Ohnishi, and R. J. H. Wokcikiewicz.** 1997. Evidence that zymogen granules are not a physiologically relevant calcium pool. Defining the distribution of inositol 1,4,5-trisphosphate receptors in pancreatic acinar cells. J. Biol. Chem. **272:**9093–9098.
58. **Vercesi, A. E., S. N. J. Moreno, and R. Docampo.** 1994. Ca^{2+}/H^+ exchange in acidic vacuoles of *Trypanosoma brucei*. Biochem. J. **304:**277–233.
59. **Vercesi, A. E., and R. Docampo.** 1996. Sodium-proton exchange stimulates Ca^{2+} release from acidocalcisomes of *Trypanosoma brucei*. Biochem. J. **315:**265–270.
60. **Vickerman, K., and L. Tetley.** 1977. Recent ultrastructural studies on trypanosomes. Ann. Soc. Belge Med. Trop. **57:**441–455.
61. **Virk, S. S., C. J. Kirk, and S. B. Shears.** 1985. Ca^{2+} transport and Ca^{2+}-dependent ATP hydrolysis by Golgi vesicles from lactating rat mammary glands. Biochem. J. **226:**741–748.
62. **Wada, Y., and Y. Anraku.** 1994. Chemiosmotic coupling of ion transport in the yeast vacuole: its role in acidification inside organelles. J. Biomembr. Bioenerg. **26:**631–637.
63. **Waldron, R. T., A. D. Short, J. J. Meadows, T. K. Ghosh, and D. L. Gill.** 1994. Thapsigargin-resistant intracellular calcium pumps. Role in calcium function and growth of thapsigargin-resistant cells. J. Biol. Chem. **269:**11927–11933.
64. **Weakly, B. S.** 1979. A variant of the pyroantimoniate technique suitable for localization of calcium in ovarian tissue. J. Histochem. Cytochem. **27:**1017–1028.
65. **Williamson, J., and D. J. MacLaren.** 1981. Localization of phosphatases in *Trypanosoma rhodesiense*. J. Protozool. **28:**460–467.
66. **Yakubu, M. A., S. Majumder, and F. Kierszenbaum.** 1994. Changes in *Trypanosoma cruzi* infectivity by treatments that affect calcium ion levels. Mol. Biochem. Parasitol. **66:**119–125.